

Nuclear Fusion of Hydrogen Isotopes Induced by the Phason Flips

in Pd and Ni Nanoclusters :

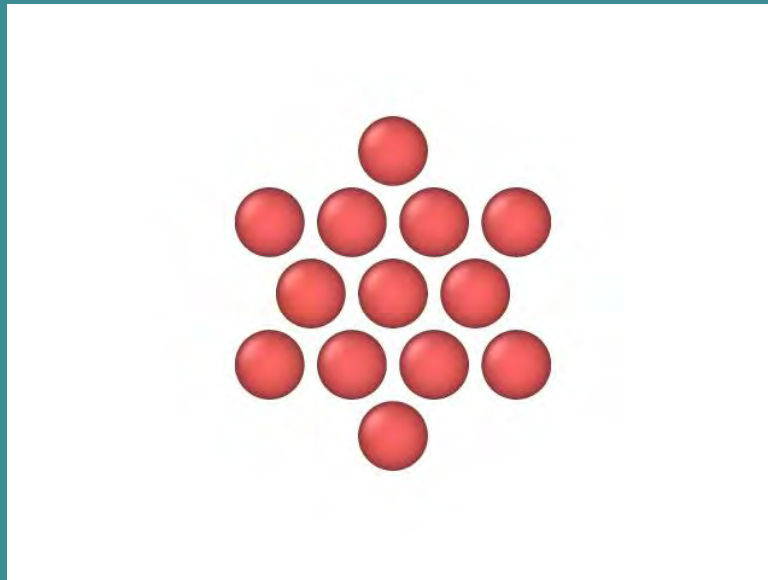
[Vladimir Dubinko](#)¹, [Denis Laptev](#)², [Dmitry Terentyev](#)³, [Klee Irwin](#)⁴

¹NSC Kharkov Institute of Physics and Technology, Ukraine

²B. Verkin Institute for Low Temperature Physics and Engineering, Ukraine

³SCK•CEN, Nuclear Materials Science Institute, Mol 2400, Belgium

⁴Quantum Gravity Research, USA



ICCF22

Outline

- Quantum tunneling induced by time-periodic driving of the potential landscape
- Discrete Breathers in Ni and Pd hydrides
- Phason Flips in Pd and Ni nanoclusters
- Phase diagram of Pd and Ni nanoclusters loaded with hydrogen
- **Low Energy Nuclear Reactions (?)**

Why LENR is unbelievable?

G. Gamow, "Zur Quantentheorie des Atomkernes", *Z. Phys.*, 51, 204–212 (1928).

$$G \approx \exp \left\{ -\frac{2}{\hbar} \int_{r_0}^{R_c} dr \sqrt{2\mu(V(r) - E)} \right\} \quad \text{Gamow factor}$$

$r_0 \sim 3 \text{ fm}$ Nuclear radius deduced from scattering experiments

$$V(R_0) = \frac{e^2}{r_0} \approx 450 \text{ keV} \quad \Rightarrow \quad \text{Coulomb barrier}$$

At any crystal
Temperature:

$$E \ll V(r_0) \Rightarrow G \approx 10^{-2760}$$

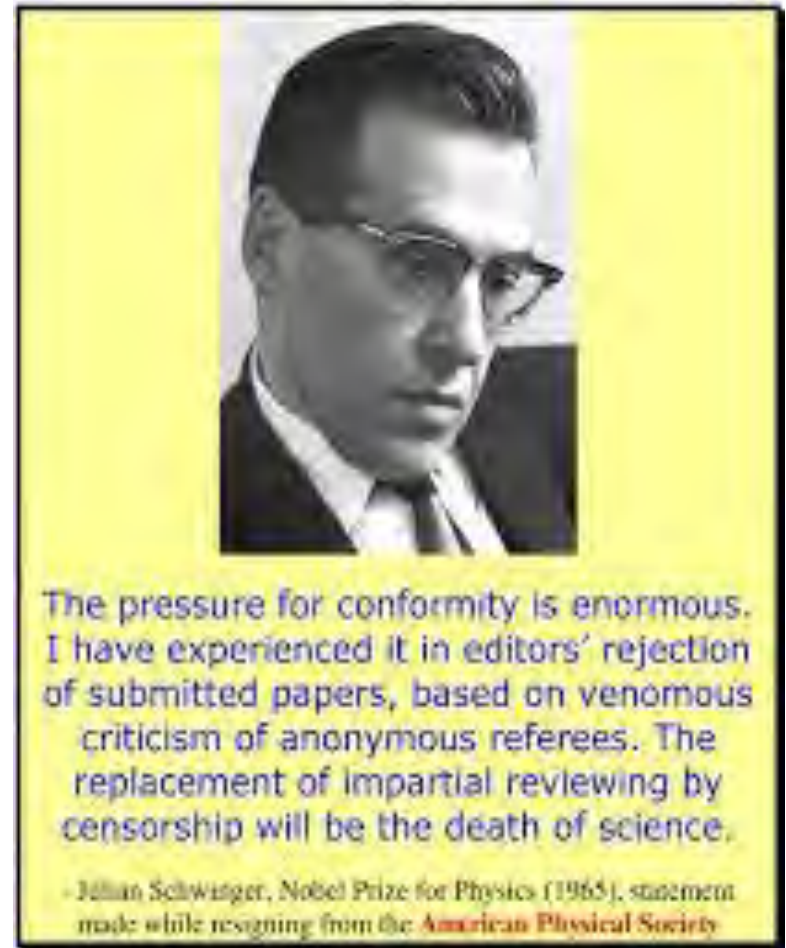
HOWEVER, is the Coulomb barrier that huge in the lattice ?

Willis Eugene *Lamb*
Nobel Prize 1955



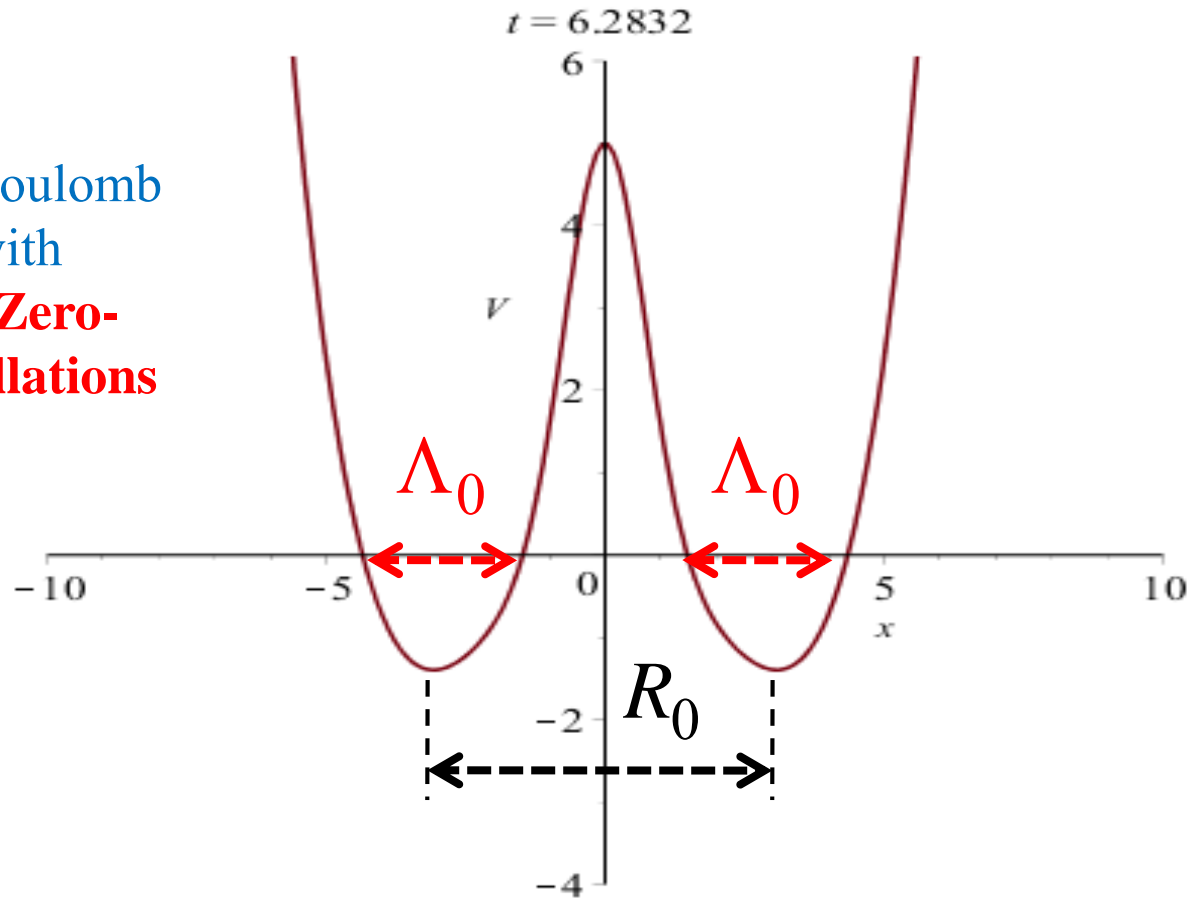
R.H. Parmenter, **W.E. Lamb**,
Cold fusion in Metals (1989)
Electron screening

Julian Schwinger
Nobel Prize 1965



J. Schwinger, **Nuclear Energy in an Atomic Lattice (1990)**
Screening due to lattice oscillations

Effective Coulomb
repulsion with
account of **Zero-
Point Oscillations**



$${}_0\langle V_c(r) \rangle_0 = \frac{e^2}{r} \sqrt{\frac{2}{\pi}} \int_0^{r/\Lambda_0} dx \exp\left(-\frac{1}{2}x^2\right) \approx \begin{cases} r \gg \Lambda_0 : \frac{e^2}{r} \\ r \ll \Lambda_0 : \left(\frac{2}{\pi}\right)^{1/2} \frac{e^2}{\Lambda_0} \sim \mathbf{100 \text{ eV} (!!!)} \end{cases}$$

J. Schwinger, *Nuclear Energy in an Atomic Lattice* The First Annual Conference on Cold Fusion. University of Utah Research Park, Salt Lake City (**1990**)

D-D fusion rate in Pd-D lattice: $\nu_{D-D} = \frac{1}{T_0} = (2\pi/\hbar)_0 \langle V \delta(H - E) V \rangle_0$

T_0 is the mean lifetime of the *phonon vacuum* state before releasing the nuclear energy **directly** to the lattice (**no radiation!**):

$$\frac{1}{T_0} \approx 2\pi\omega_0 \left(\frac{2\pi\hbar\omega_0}{E_{nucl}} \right)^{\frac{1}{2}} \left(\frac{r_{nucl}}{\Lambda_0} \right)^3 \exp \left[-\frac{1}{2} \left(\frac{R_0}{\Lambda_0} \right)^2 \right] \sim 10^{-19} s^{-1} \div 10^{-30} s^{-1}$$

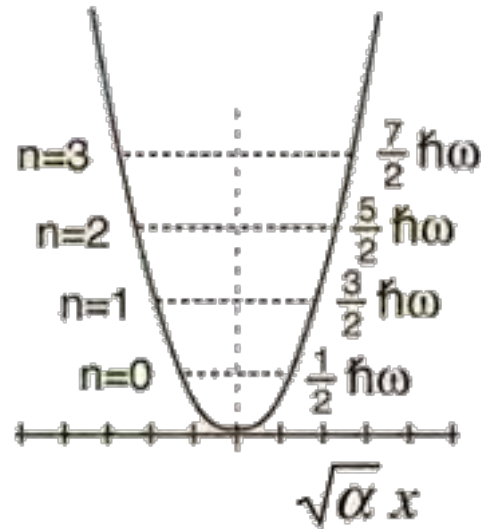
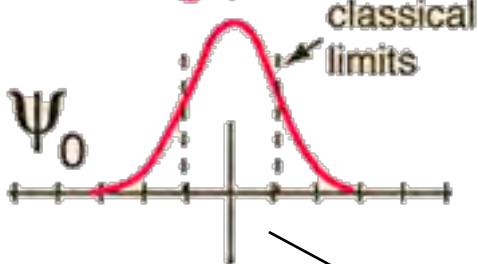
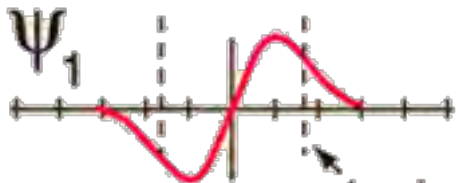
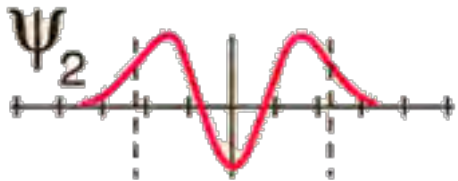
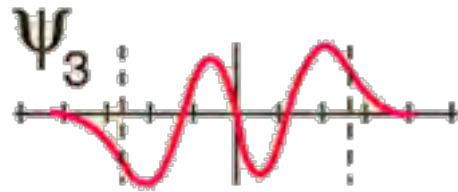
$\Lambda_0 = 0.1\text{\AA}$
 $R_0 = 0.94\text{\AA} \div 2.9\text{\AA}$

When we heat the system we increase temperature, i.e. we increase the *thermal* noise strength

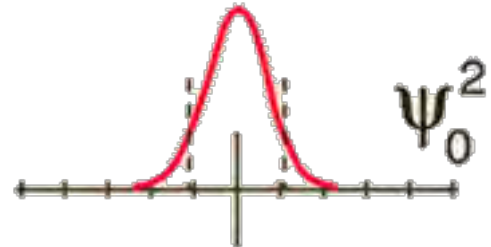
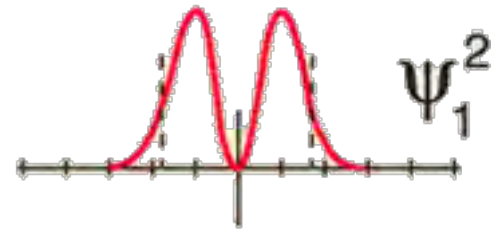
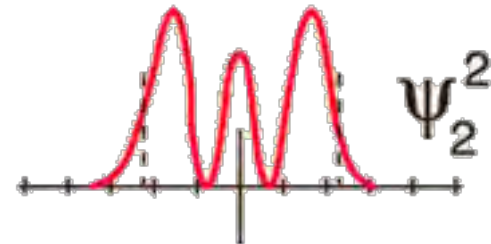
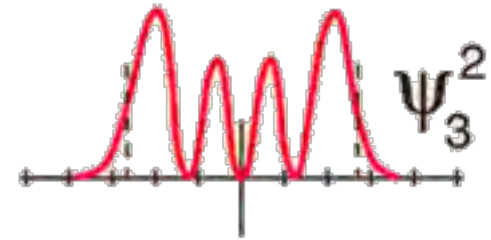
Can we increase the *quantum* noise strength, i.e. ZPO energy and amplitude?

Stationary harmonic potential

$$\langle E \rangle_n = \hbar\omega_0 \left(n + \frac{1}{2} \right)$$

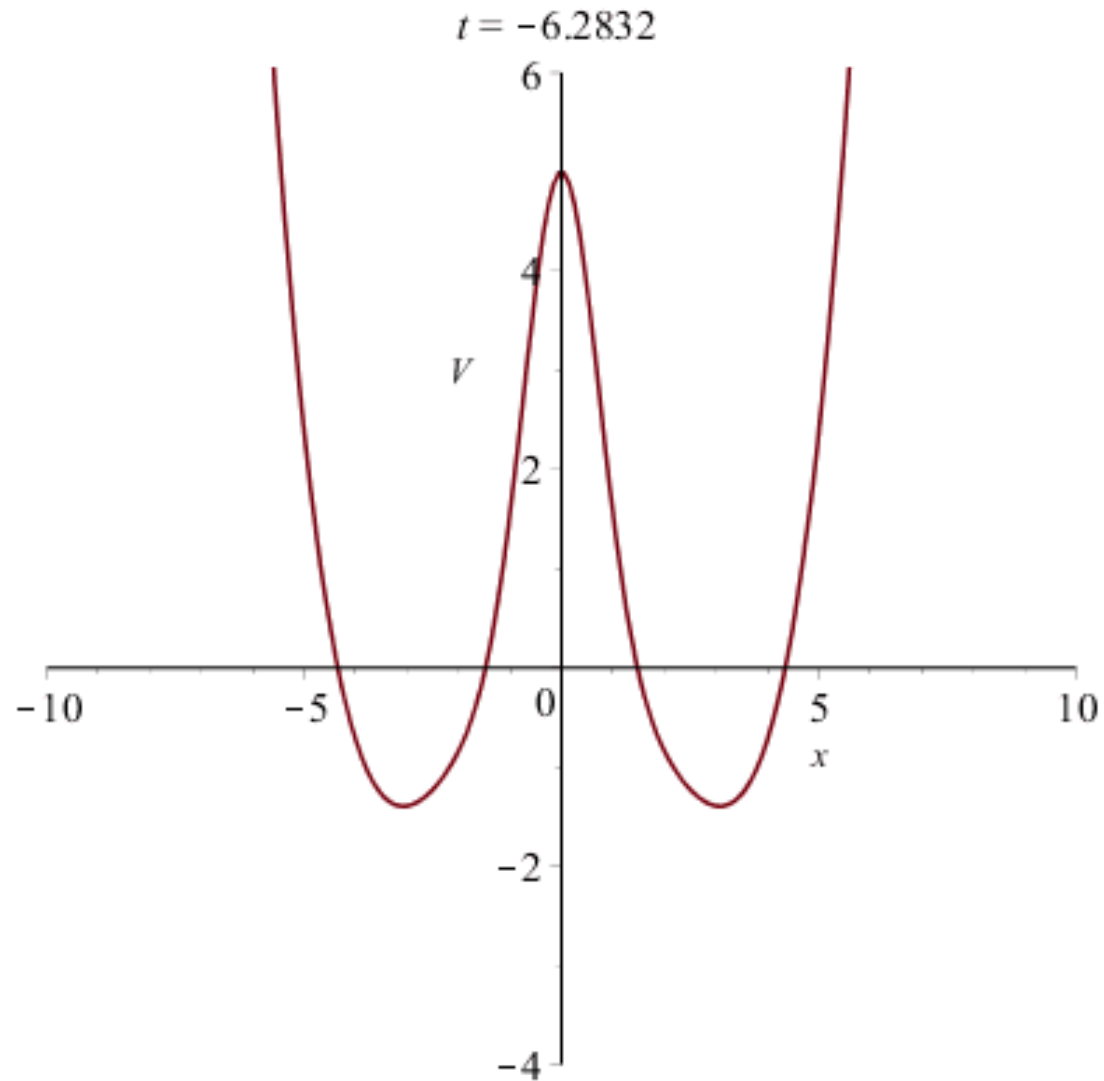


Harmonic oscillator potential and wavefunctions



$$E_{ZPO} = \frac{\hbar\omega_0}{2}$$

Time-periodic modulation of the **double-well** shape changes (i) eigenfrequency and (ii) position of the wells



Parametric resonance with time-periodic eigenfrequency $\Omega = 2\omega_0$

$$i\hbar \frac{\partial \psi}{\partial t} = -\frac{\hbar^2}{2m} \frac{\partial^2 \psi}{\partial x^2} + \frac{m\omega^2(t)}{2} x^2 \psi$$

Schrödinger equation

$$\psi(x_0, t_0 = 0) = \frac{1}{\sqrt[4]{2\pi\sigma_0}} \exp\left(-\frac{x_0^2}{4\sigma_0}\right)$$

Initial Gaussian packet $\sigma_0 = \frac{\hbar}{2m\omega_0}$

Parametric regime $\Omega = 2\omega_0$:

$$\ddot{x} + \omega_0^2 [1 - g \cos(2\omega_0 t)] x = 0$$

$g \ll 1$ – modulation amplitude

$$\sigma_x(t) = \sigma_0 \cosh\left(\frac{g\omega_0 t}{2}\right) \left[1 + \tanh\left(\frac{g\omega_0 t}{2}\right) \sin(2\omega_0 t) \right] \quad \text{dispersion}$$

ZPO energy:

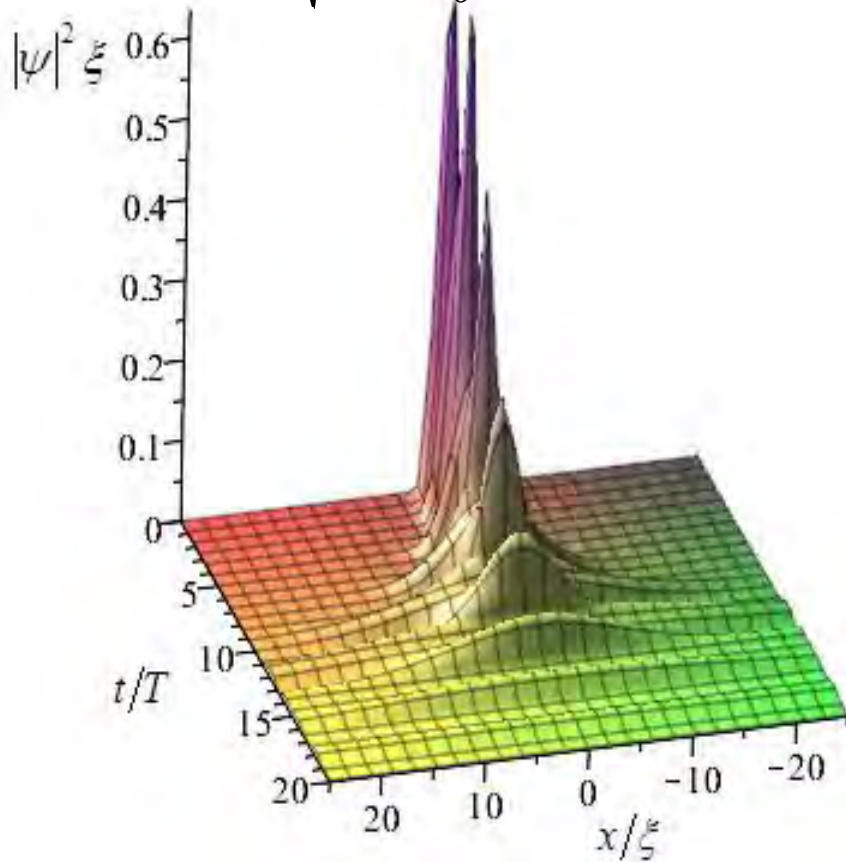
$$\langle E \rangle = \frac{1}{2m} \sigma_p + \frac{m\omega^2(t)}{2} \sigma_x = \frac{\hbar\omega_0}{2} \cosh \frac{g\omega_0 t}{2}$$

ZPO amplitude:

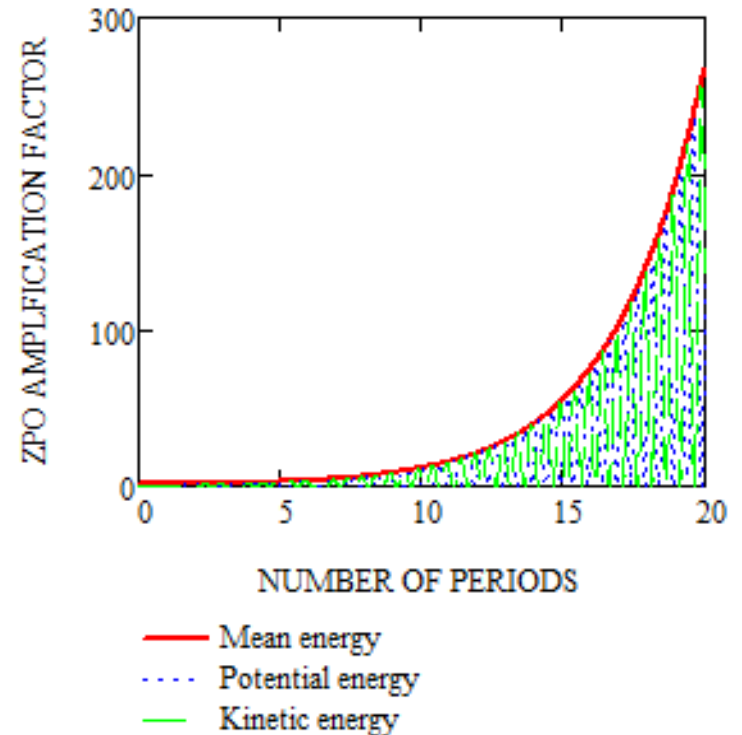
$$\Lambda_{ZPO}(t) = \sqrt{\frac{\hbar}{2m\omega_0} \cosh \frac{g\omega_0 t}{2}}$$

Non-stationary harmonic potential with time-periodic eigenfrequency $\Omega = 2\omega_0$

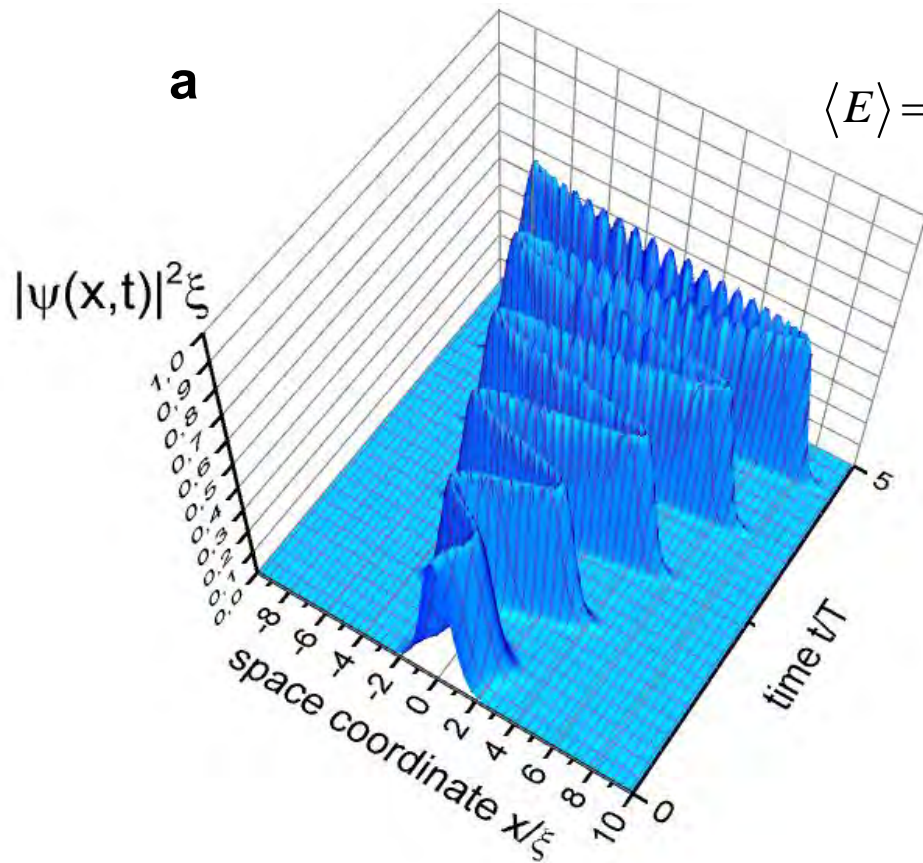
$$\Lambda_{ZPO}(t) = \sqrt{\frac{\hbar}{2m\omega_0} \cosh \frac{g\omega_0 t}{2}}$$



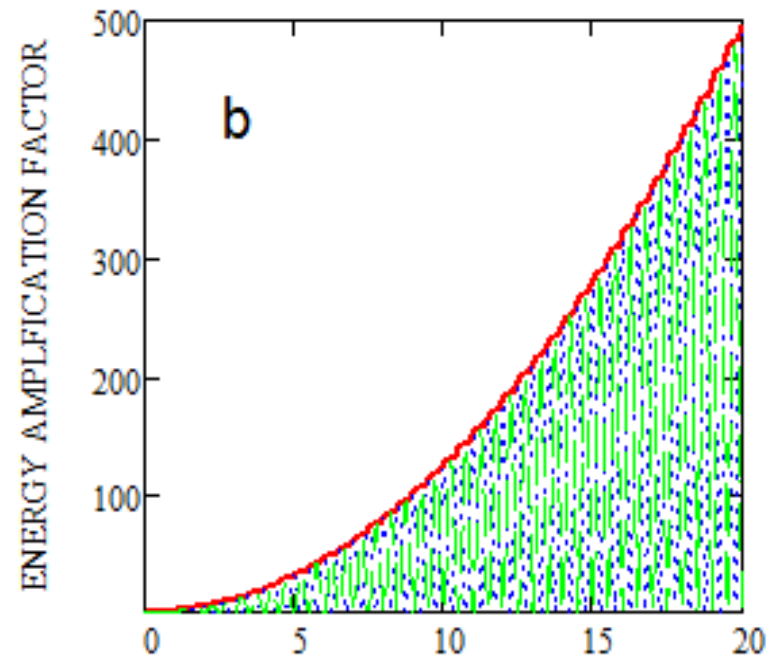
$$E_{ZPO}(t) = \frac{\hbar\omega_0}{2} \cosh \frac{g\omega_0 t}{2}$$



Non-stationary harmonic potential with time-periodic shifting of the well position at $\Omega = \omega_0$



$$\langle E \rangle = \frac{\hbar\omega_0}{2} + \frac{(g_A A_{ZPO})^2 m\omega_0^2}{8} \left[\omega_0^2 t^2 + \omega_0 t \sin 2\omega_0 t + \sin^2 \omega_0 t \right]$$



$$\lambda(t) = \frac{g_A A_{ZPO}}{2} \omega_0 t \left(\cos \omega_0 t - \frac{\sin \omega_0 t}{\omega_0 t} \right)$$

NUMBER OF PERIODS

- Mean energy
- ⋯ Potential energy
- Kinetic energy

Numerical solution of non-stationary Schrodinger Equation

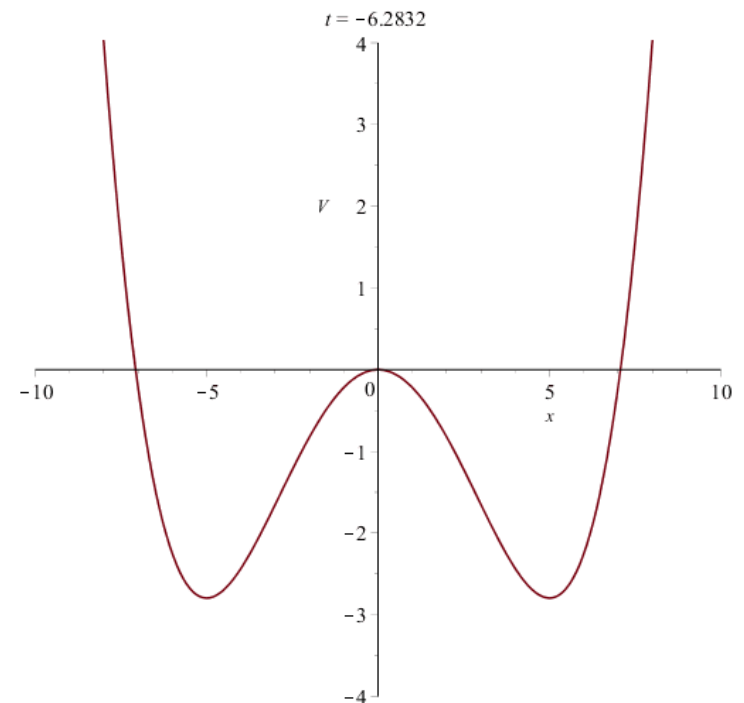
$$i\hbar \frac{\partial}{\partial t} \psi(x,t) = -\frac{\hbar^2}{2m} \frac{\partial^2}{\partial x^2} \psi(x,t) + V(x,t) \psi(x,t)$$

Time-periodic double-well potential:

$$V(x,t) = \frac{\hbar\omega_0}{2} \left[a(t) \left(\frac{x}{\xi} \right)^4 - b(t) \left(\frac{x}{\xi} \right)^2 \right] = \frac{\hbar\omega_0}{2} u(\tilde{x}, \tau)$$

$$a(t) = \frac{\alpha - \beta \cos(\varepsilon\omega_0 t)}{2\sqrt{\alpha}}, \quad b(t) = \frac{\sqrt{\alpha - \beta \cos(\varepsilon\omega_0 t)}}{2\sqrt{\alpha}}$$

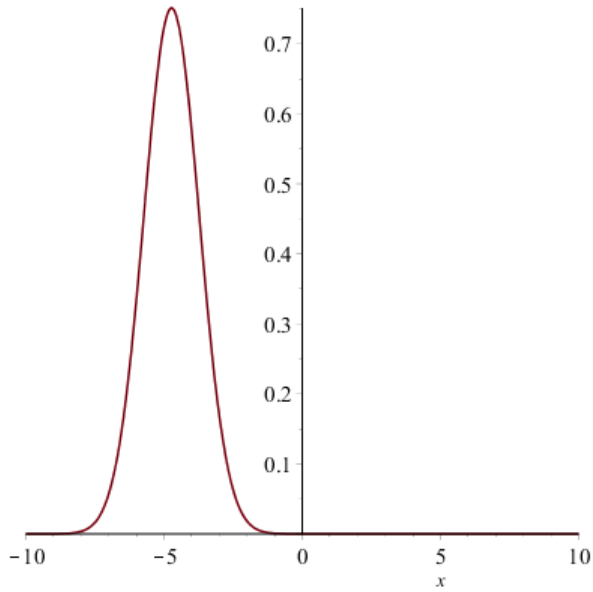
$$\varepsilon = 1 \div 2,$$



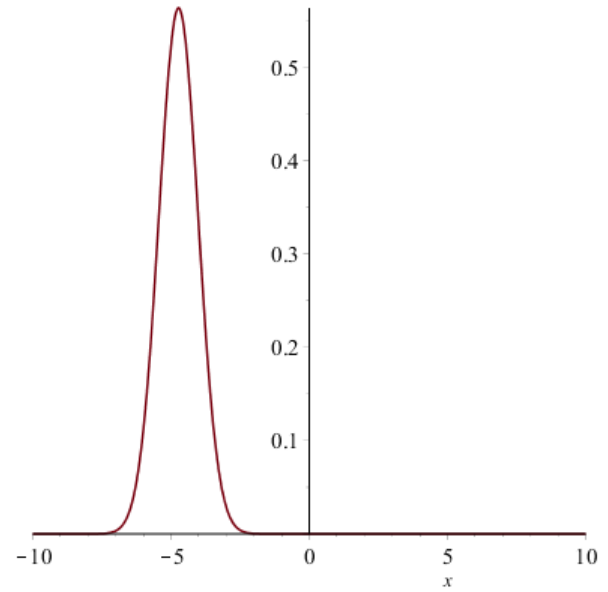
Initial condition: Gauss wave function

$$\psi_R(\tilde{x}, 0) = \begin{cases} \frac{1}{\sqrt[4]{\pi\xi^2}} \exp\left(-\frac{1}{2}(\tilde{x} - \tilde{S}_x)^2\right), & -N < \tilde{x} < +N \\ 0, & |\tilde{x}| \geq N \end{cases}, \psi_I(\tilde{x}, 0) = 0$$

$$\tilde{S}_x = \tilde{x}_{\min}^{(-)} = -\frac{1}{\sqrt{2}\sqrt[4]{\alpha}}$$

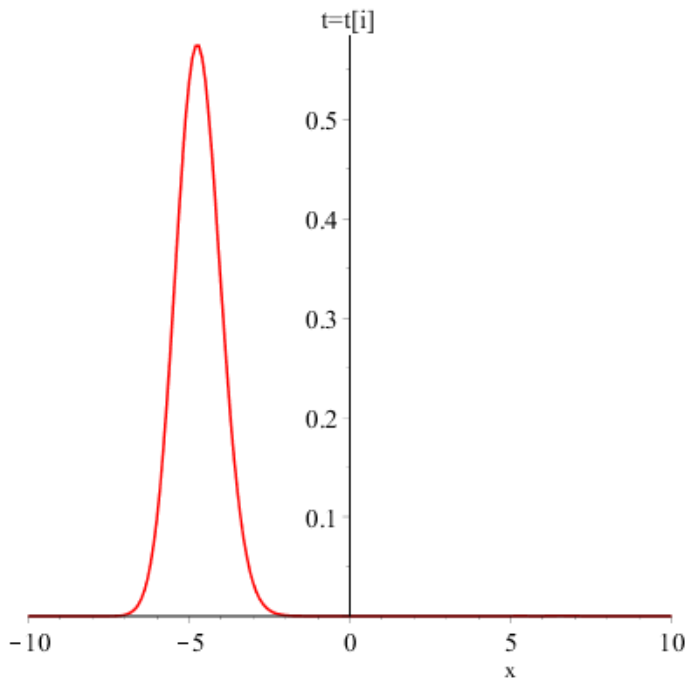


Initial wave function



Initial probability density

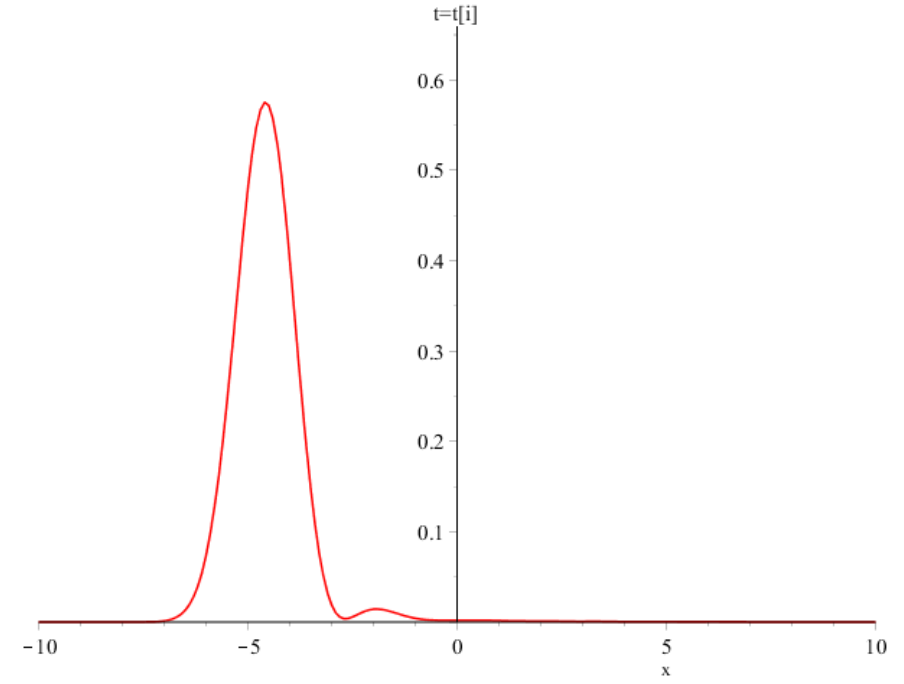
$\alpha = 0.0005$ $\beta = 0.0$



Stationary double-well
potential

0-500T

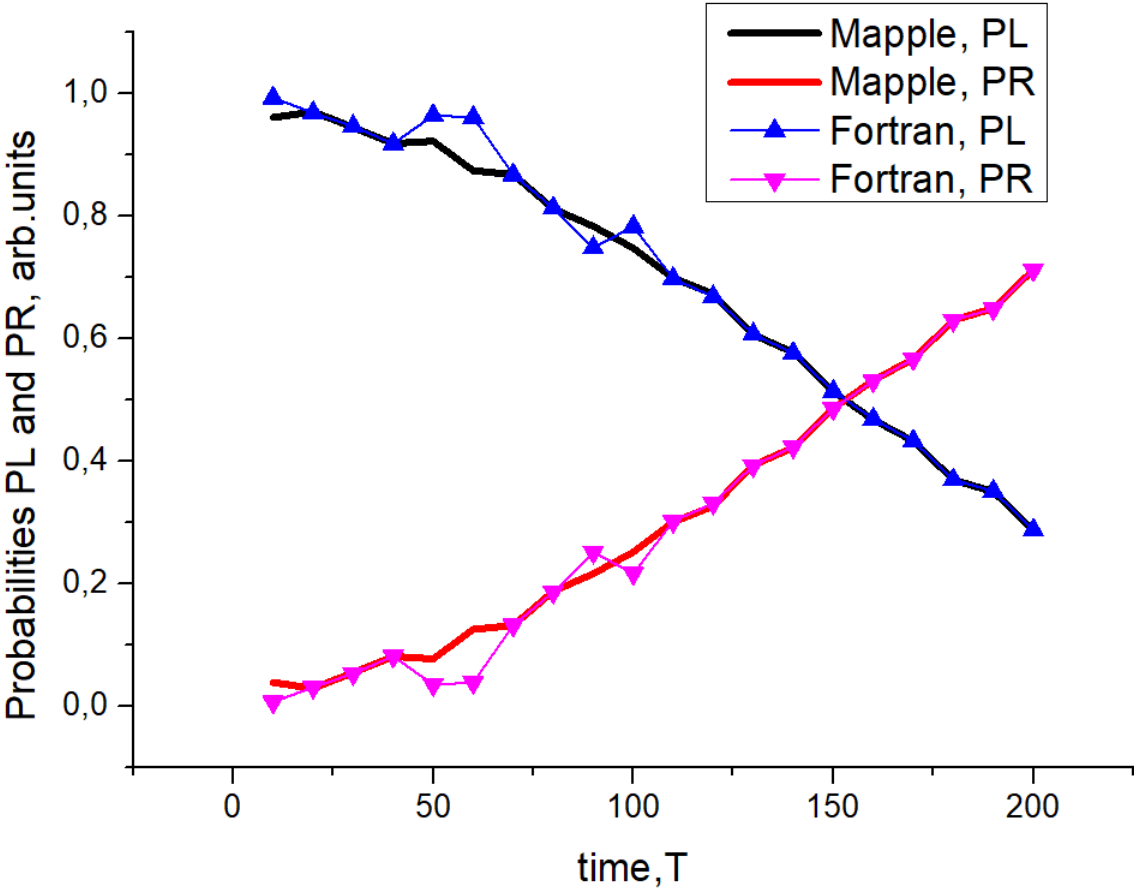
$\alpha = 0.0005$ $\beta = 0.0001$



Non-Stationary double-well potential

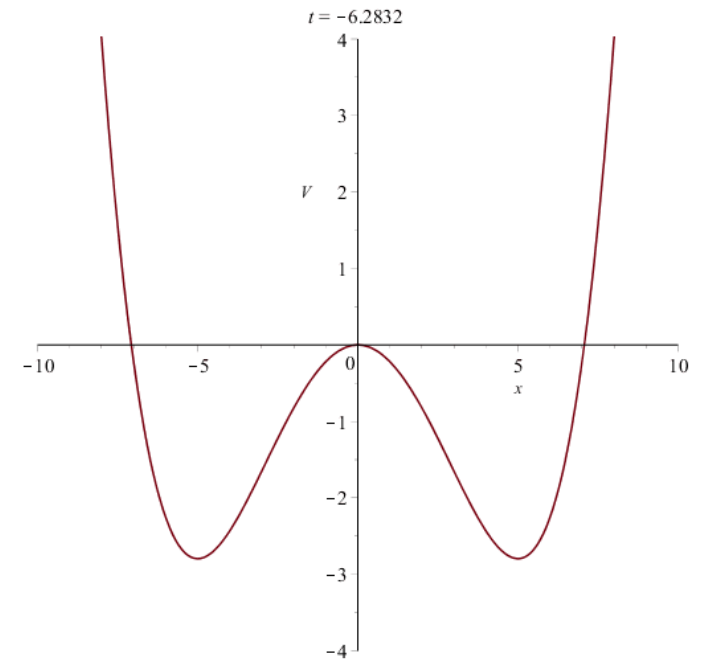
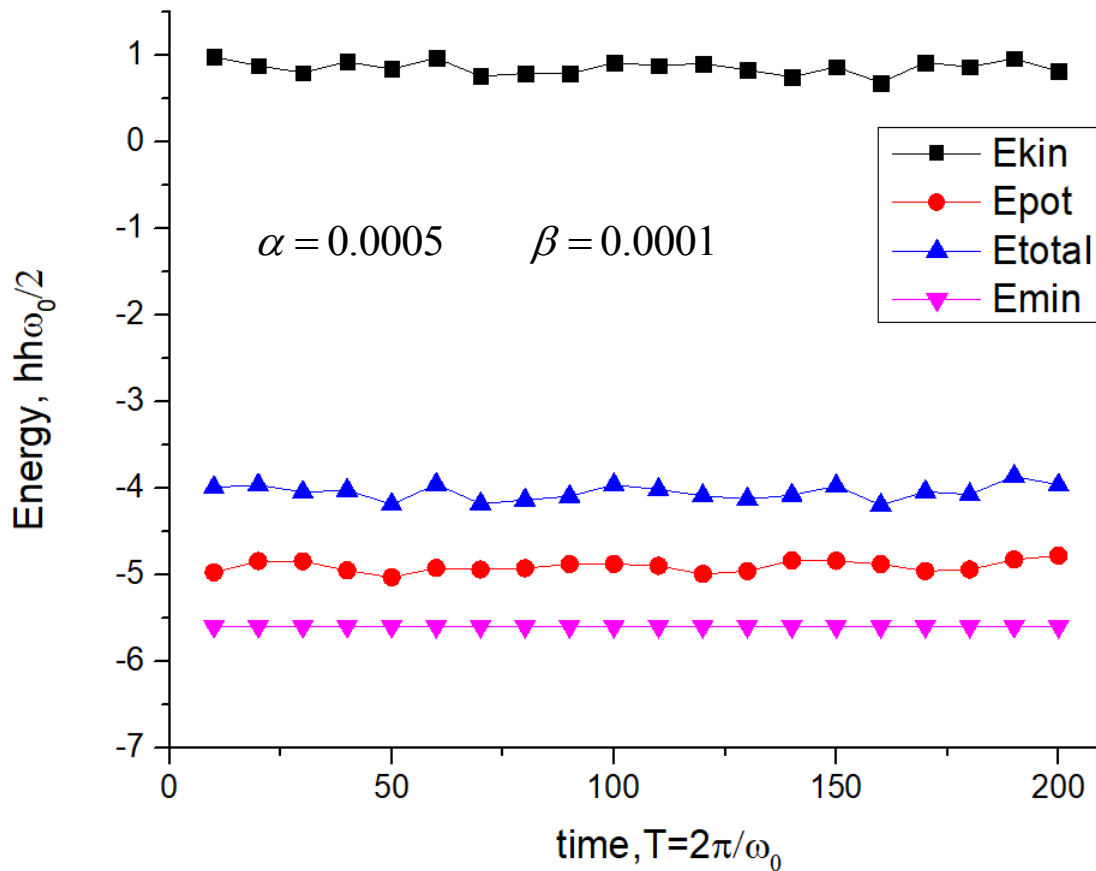
0-500T

Probabilities to find a particle in the left (PL) or right (PR) well for the case of the Nonstationary double-well potential



Energy evolution in time-periodic double-well potential:

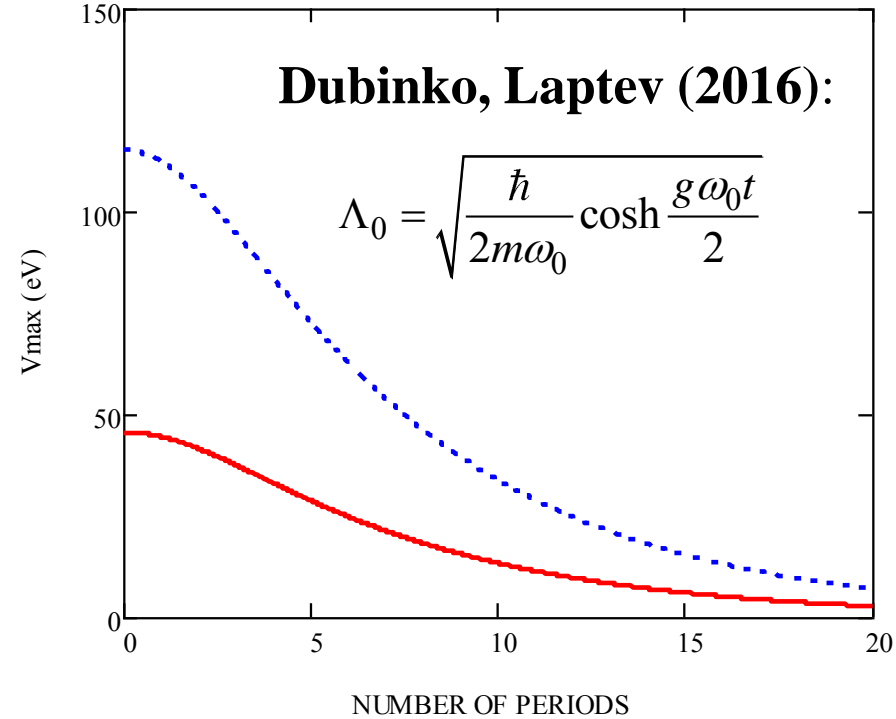
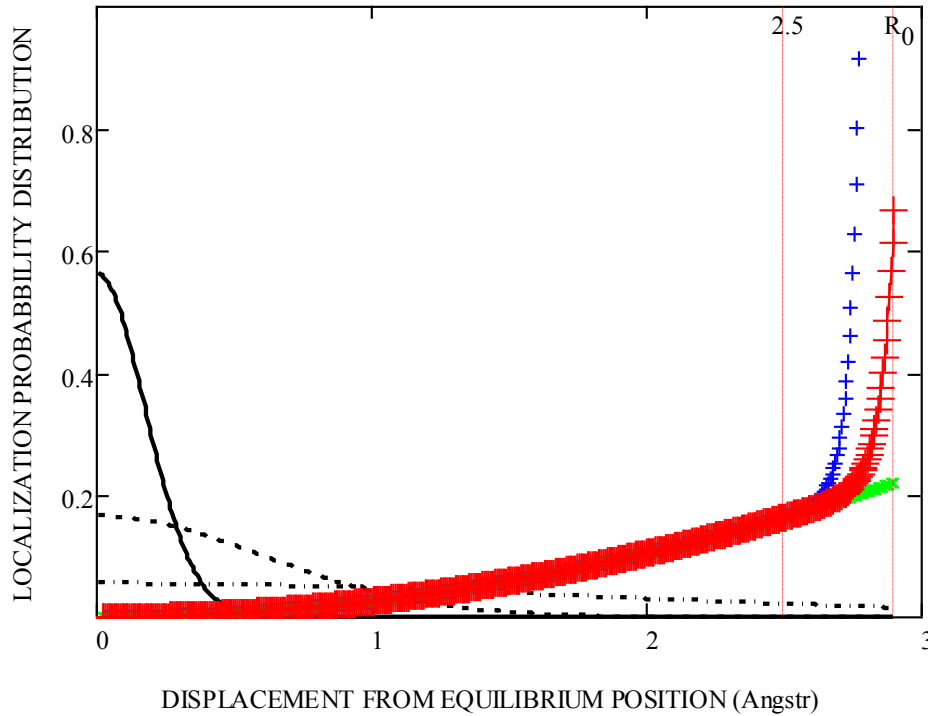
$$\sigma_x = \left\langle (x - \langle x \rangle)^2 \right\rangle, \quad \sigma_p = \left\langle (p - \langle p \rangle)^2 \right\rangle, \quad \langle E \rangle = \frac{1}{2m} \sigma_p + \frac{m\omega^2(t)}{2} \sigma_x$$



Schwinger, **Nuclear Energy in an Atomic Lattice** I, Z. Phys. D 15, 221 (1990).

Parmenter, Lamb, **Cold fusion in Metals**, Proc. Natl. Acad. Sci. USA, v. 86, 8614-8617 (1989).

$$V_{eff}(r) \approx \frac{m\omega_0^2}{2} r^2 + \frac{e^2}{R_0 - r} \exp\left(-\frac{R_0 - r}{\lambda_D}\right) \sqrt{\frac{2}{\pi}} \int_0^{(R_0 - r)/\Lambda_0} dx \exp\left(-\frac{1}{2} x^2\right)$$



- N=0
- - - N=10
- · · N=17
- +++ Effective potential (x10 eV) by eq. (44) [P&L]
- x x x Harmonic potential (x10 eV)
- + + + Effective potential (x10 eV) at N=17 by eq. (45) [Schwinger]

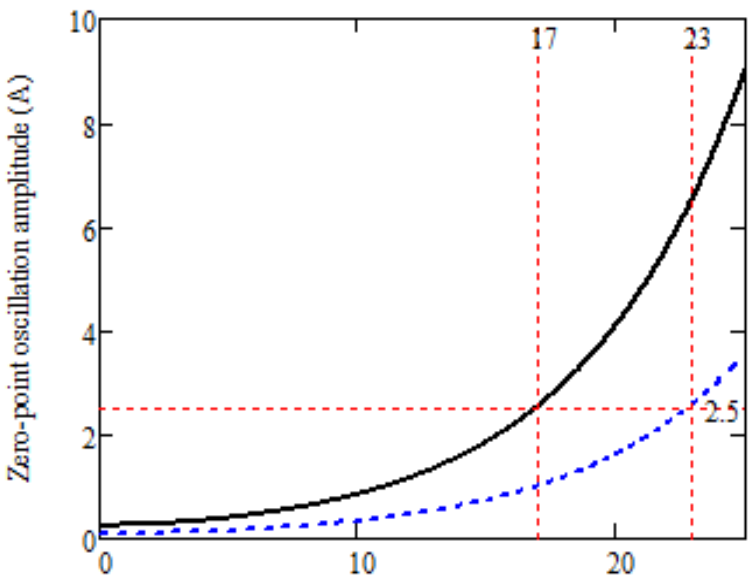
- w₀=50 THz (Rowe et al [19])
- · · w₀=320 THz (Schwinger [21])

Schwinger, *Nuclear energy in an atomic lattice*. Proc. Cold Fusion Conf. (1990)

Dubinko, Laptev, *Chemical and nuclear catalysis driven by LAVs*, LetMat (2016)

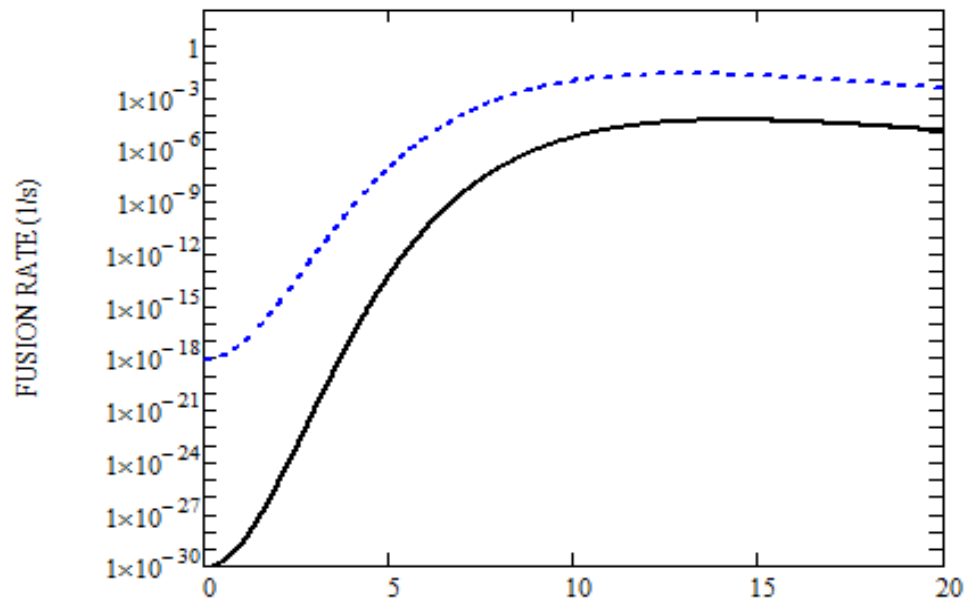
$$\frac{1}{T} \approx 2\pi\omega_0 \left(\frac{2\pi\hbar\omega_0}{E_{nucl}} \right)^{\frac{1}{2}} \left(\frac{r_{nucl}}{\Lambda} \right)^3 \exp \left[-\frac{1}{2} \left(\frac{R_0}{\Lambda_0} \right)^2 \right]$$

$$\Lambda_0 = \left\{ \begin{array}{l} \sqrt{\frac{\hbar}{2m\omega_0}} = const \\ \sqrt{\frac{\hbar}{2m\omega_0} \cosh \frac{g\omega_0 t}{2}} \end{array} \right.$$



NUMBER OF PERIODS

— w0= 50 THz (Rowe et al [19])
 - - - w0=320THz (Schwinger [21])



NUMBER OF PERIODS

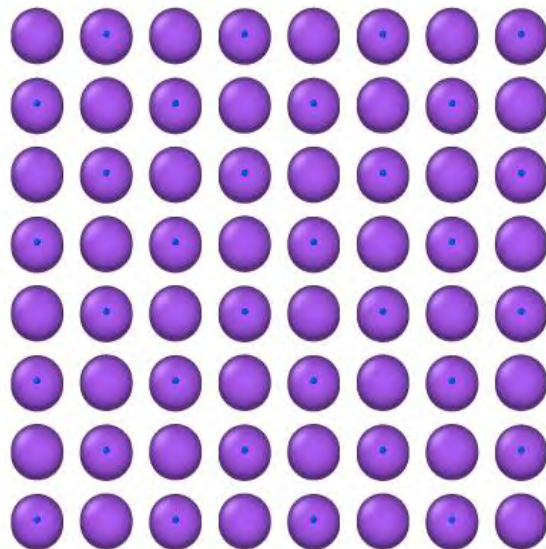
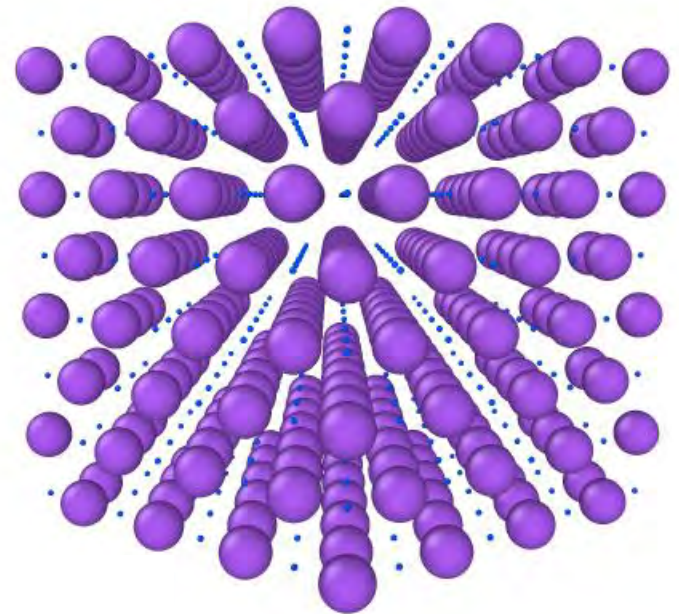
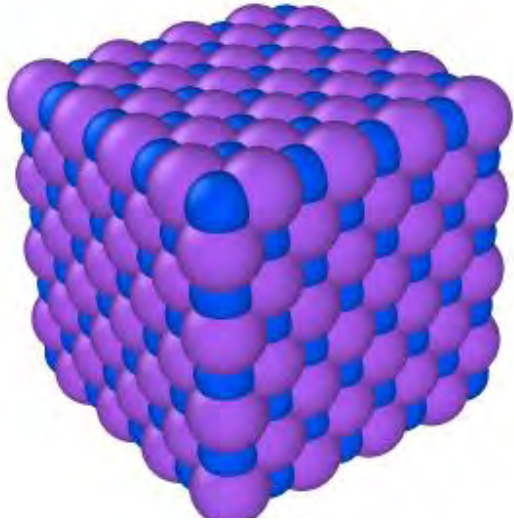
— w0=50 THz; PdD: R0=2.9A
 - - - w0=320 THz; PdD2: R0=0.94A (Schwinger)

In order to increase probability of nuclear fusion we need a mechanism of time-periodic driving of the potential landscape

- **Discrete Breathers in periodic crystals**
- **Phasons Flips in nanocrystals**
- **etc**

MD modeling of DBs in NiH and PdH crystals

Visualization of the Pd(Ni)H fcc Lattice (NaCl type)

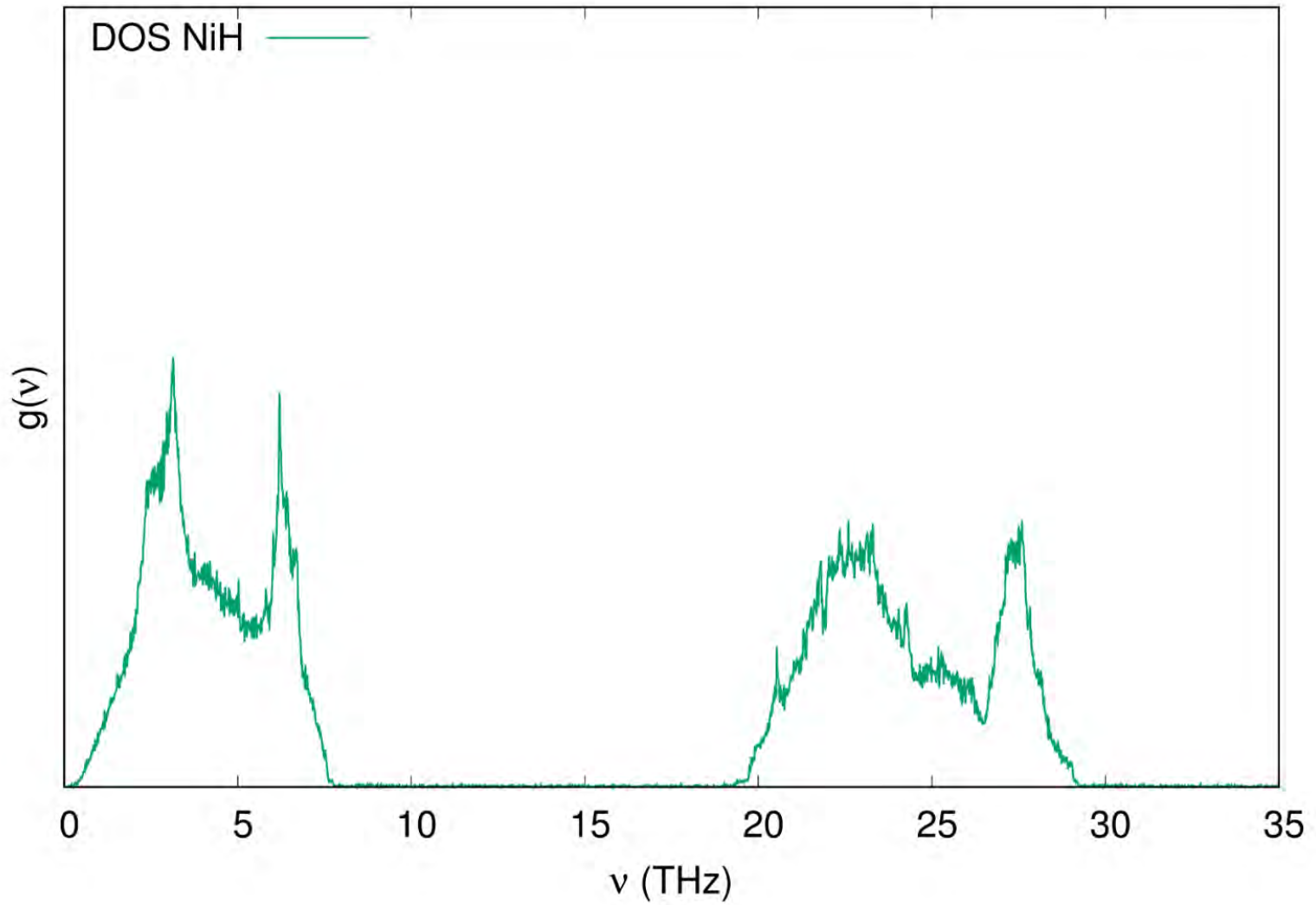


NiH lattice

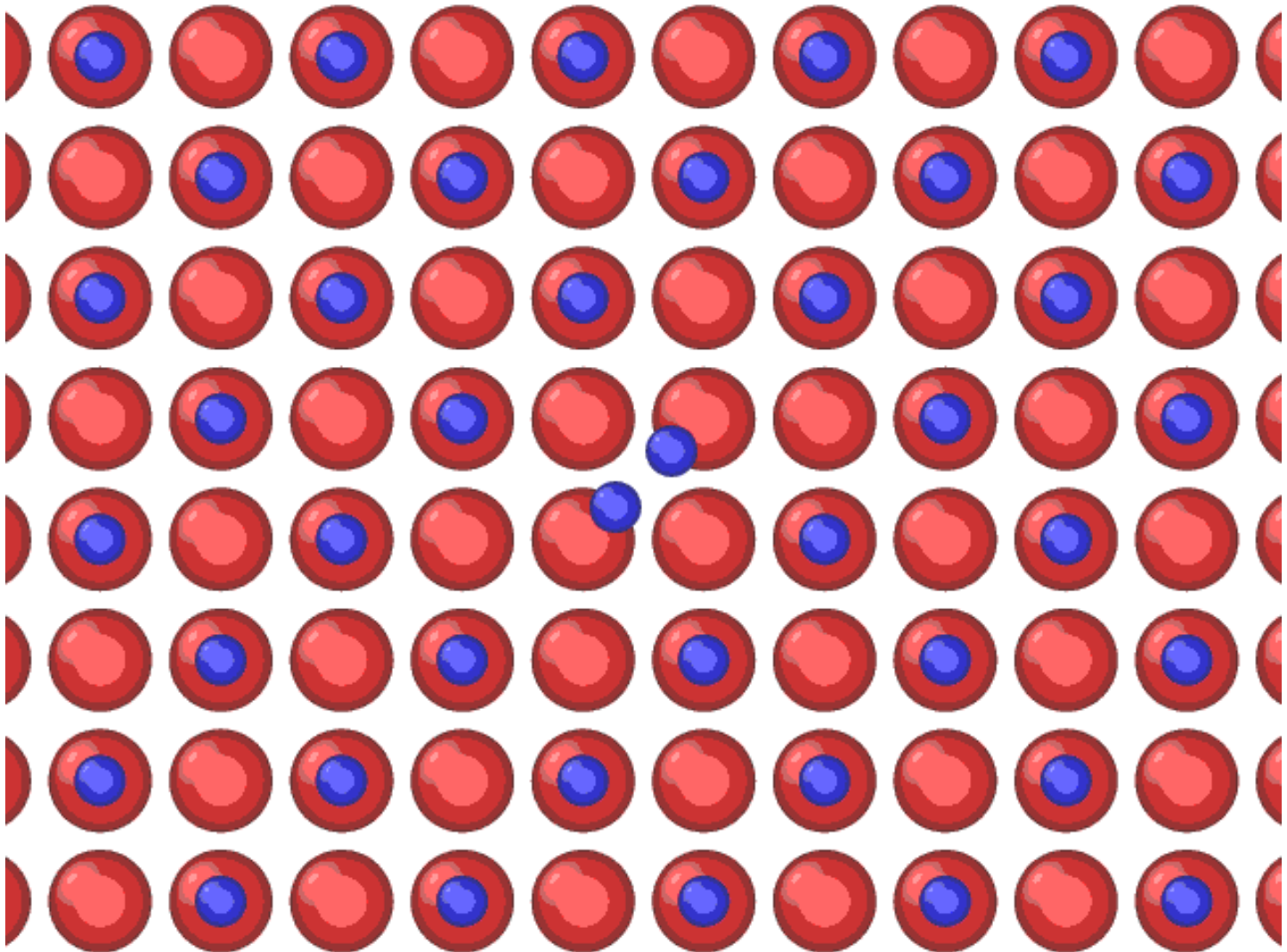
The following potential was used for Ni lattice modeling in **LAMMPS** package:

Material	File with potential used	The link to the corresponding publication in the literature
NiH	NiAlH_jea.eam.alloy	see James E Angelo, Neville R Moody, Michael I Baskes"Trapping of hydrogen to lattice defects in nickel", Modelling and Simulation in Materials Science & Engineering, vol. 3, pp. 289-307 (1995)

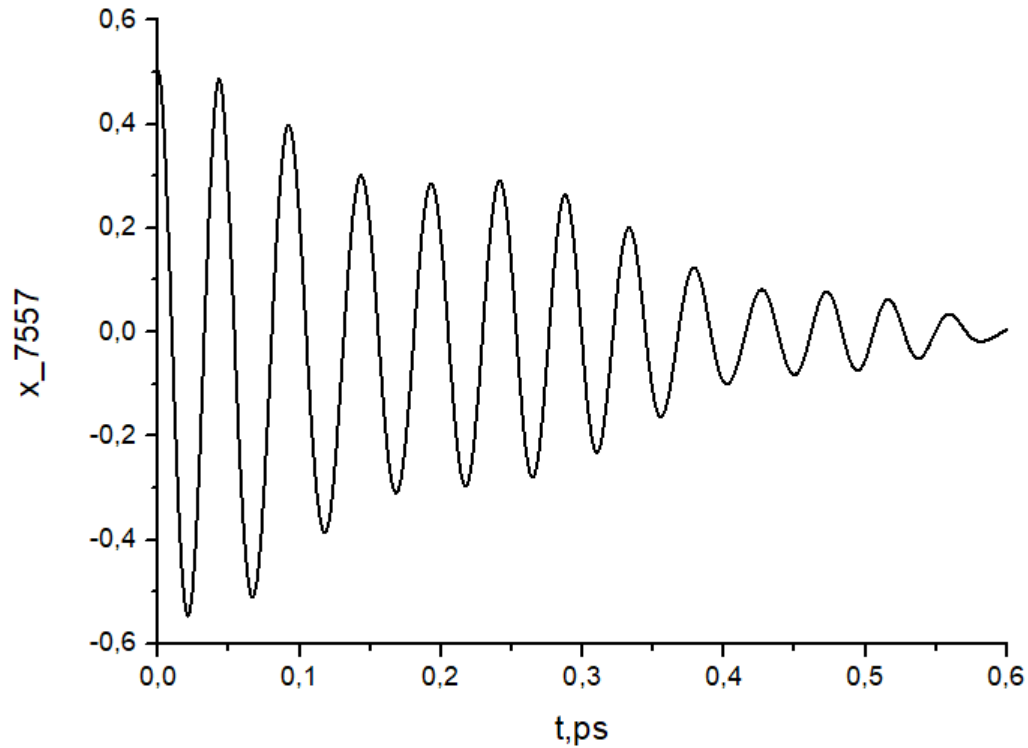
Density Of States of NiH at 0 K



H-H atoms displaced along $[110]$ in NiH at $T=0\text{K}$

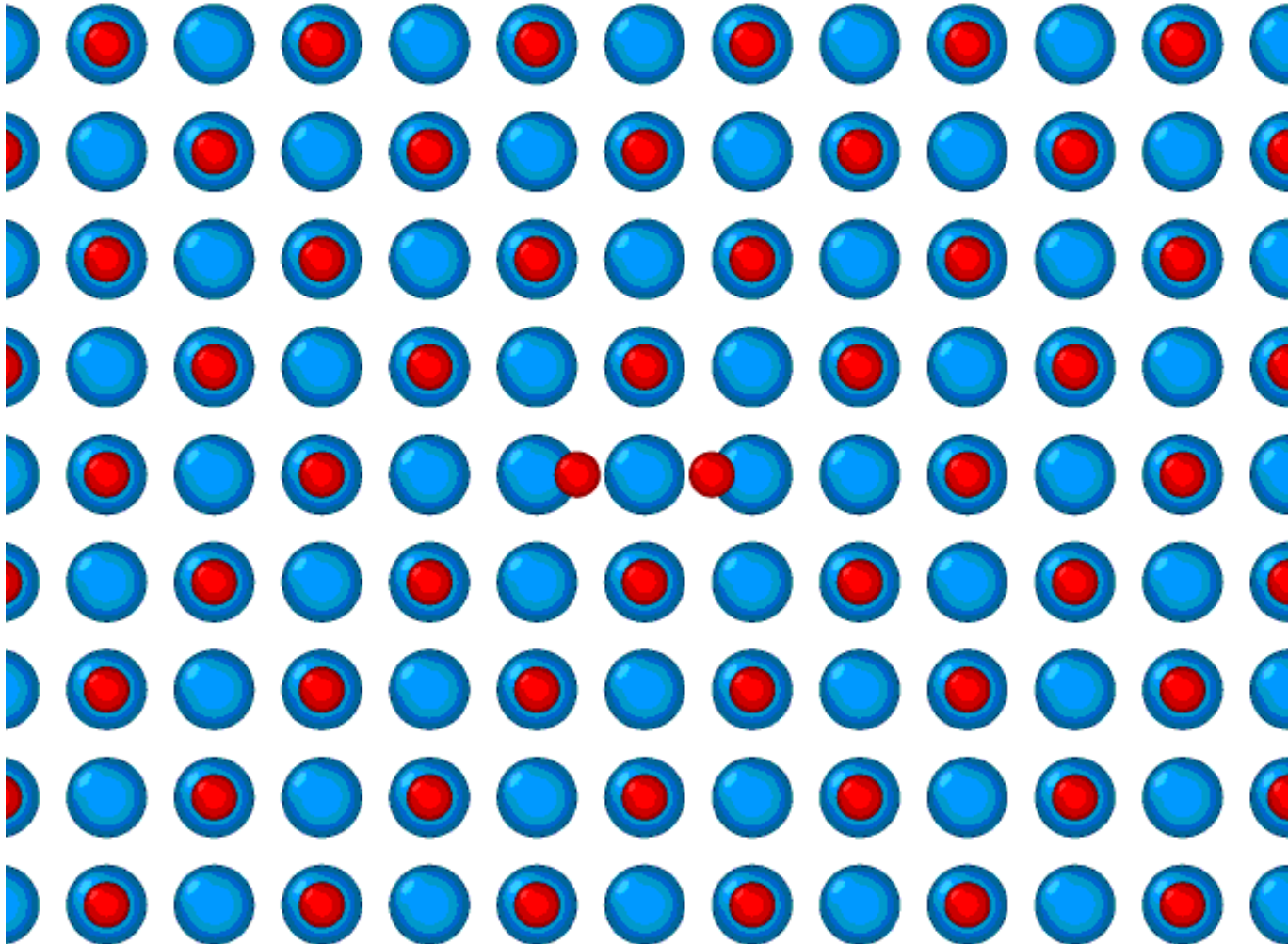


1 H atom displaced along $\langle 110 \rangle$ in NiH at $T=0K$

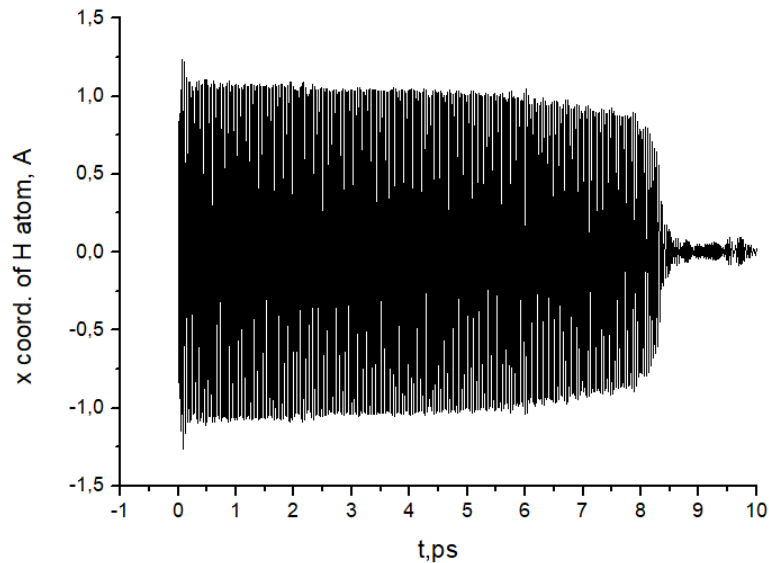


$T=0.5$ ps, Frequency = 20THz (**inside** the optical band)

H-Ni-H atoms [100] and [-100] in NiH at T=0K

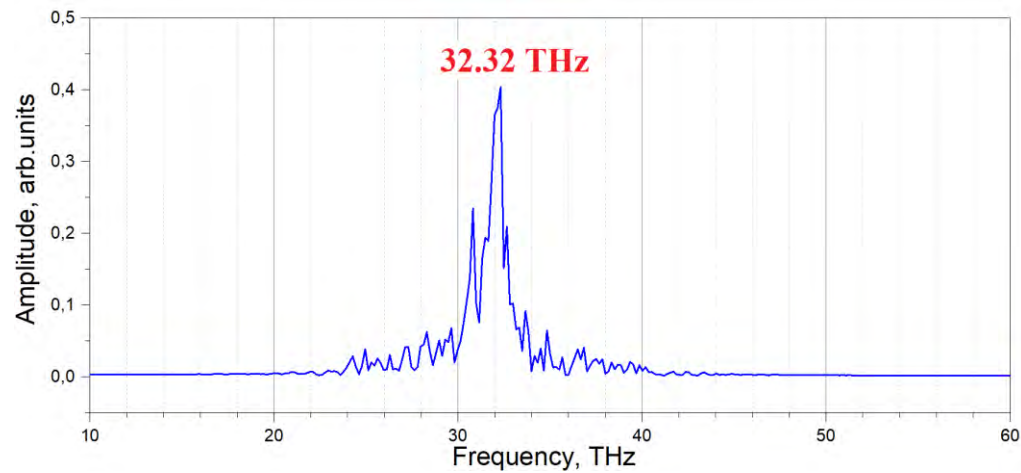


H-Ni-H DB in NiH with [100] polarization



Amplitude = 1.05 Å

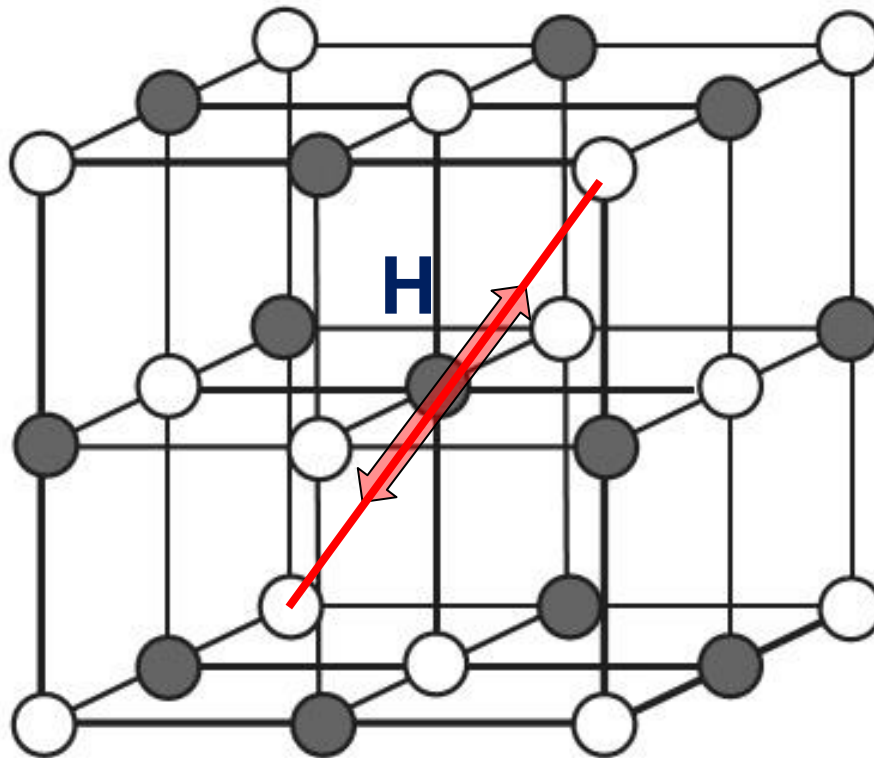
Frequency = 32.32 THz



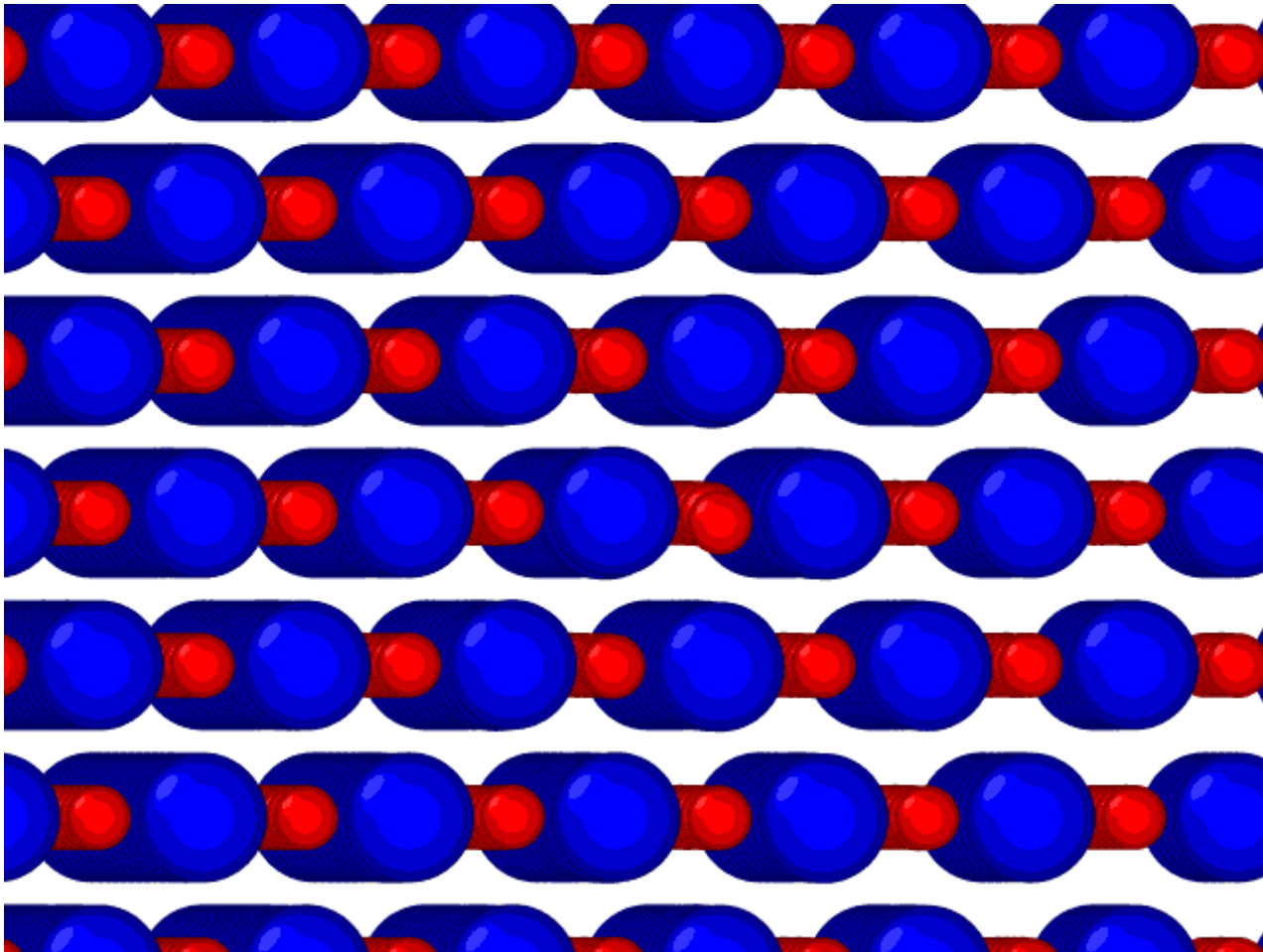
Period = 0.03 ps

Lifetime = 8.3 ps = 271(T)

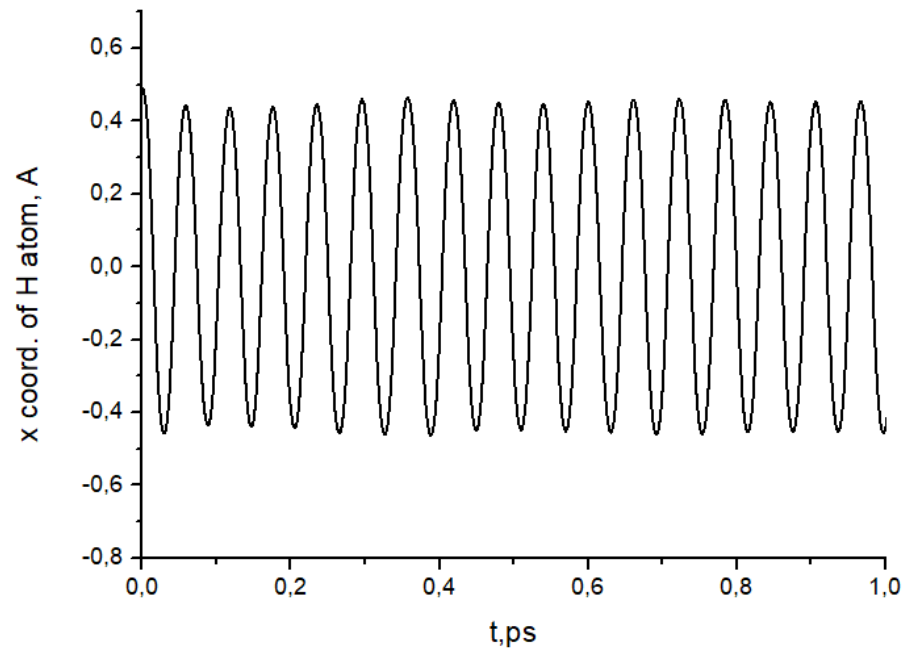
Excitation of DB with [111] polarization in NiH



DB with [111] polarization in NiH



DB in NiH with [111] polarization



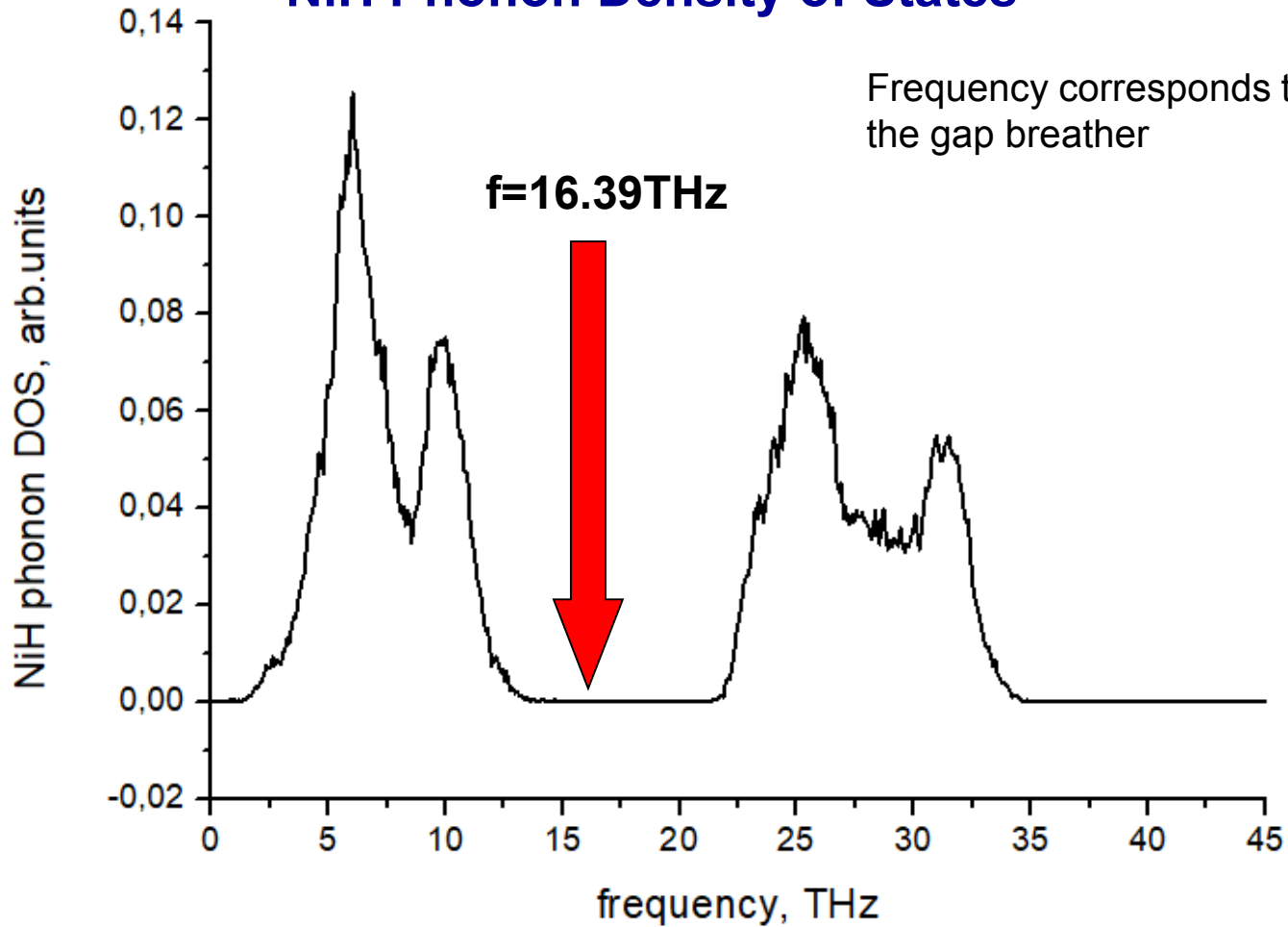
Amplitude = 0.79 A

Period = 0.061 ps

Frequency = 16.39 THz

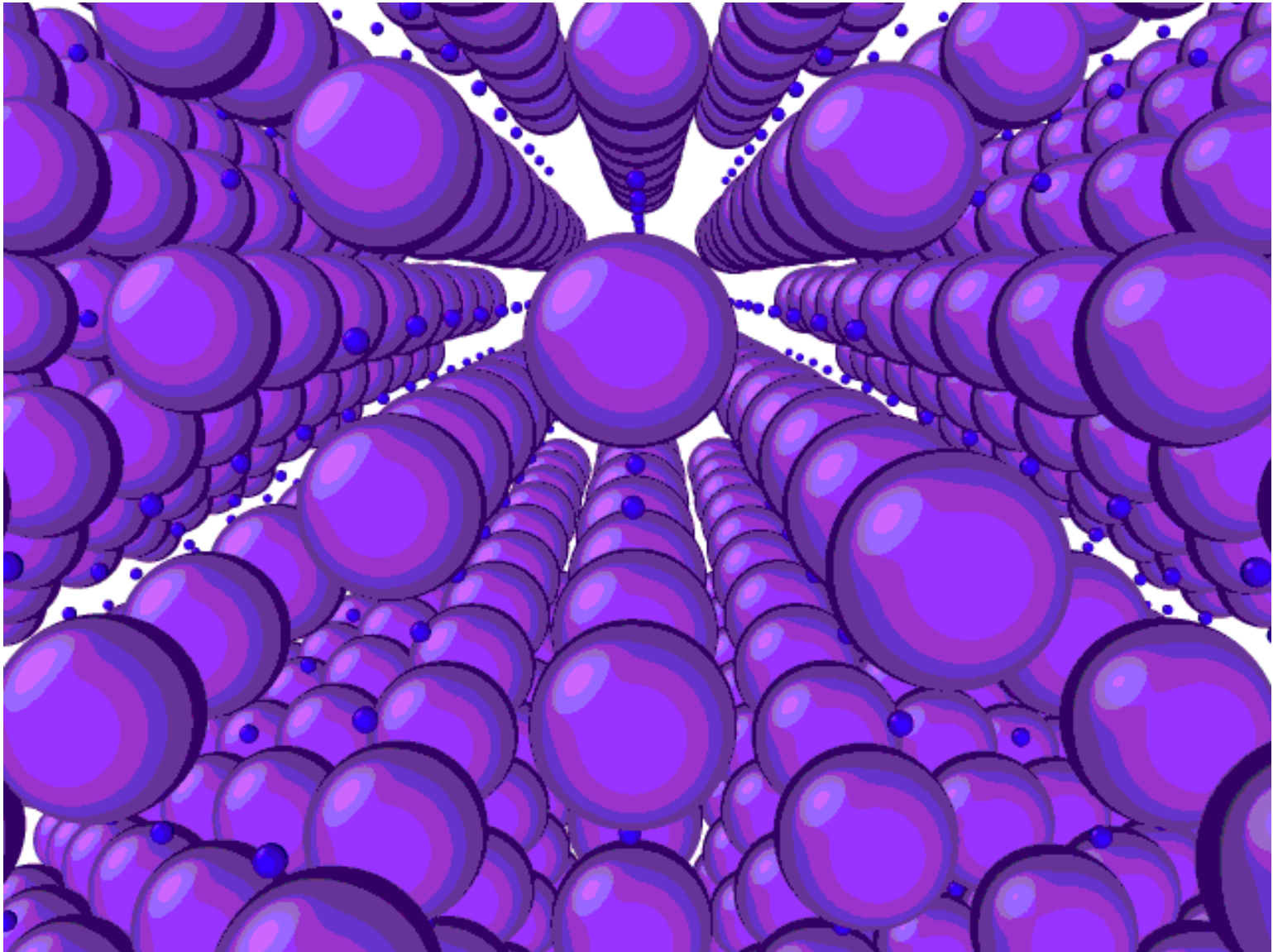
Lifetime > 417 ps = 6836(T)

NiH Phonon Density of States

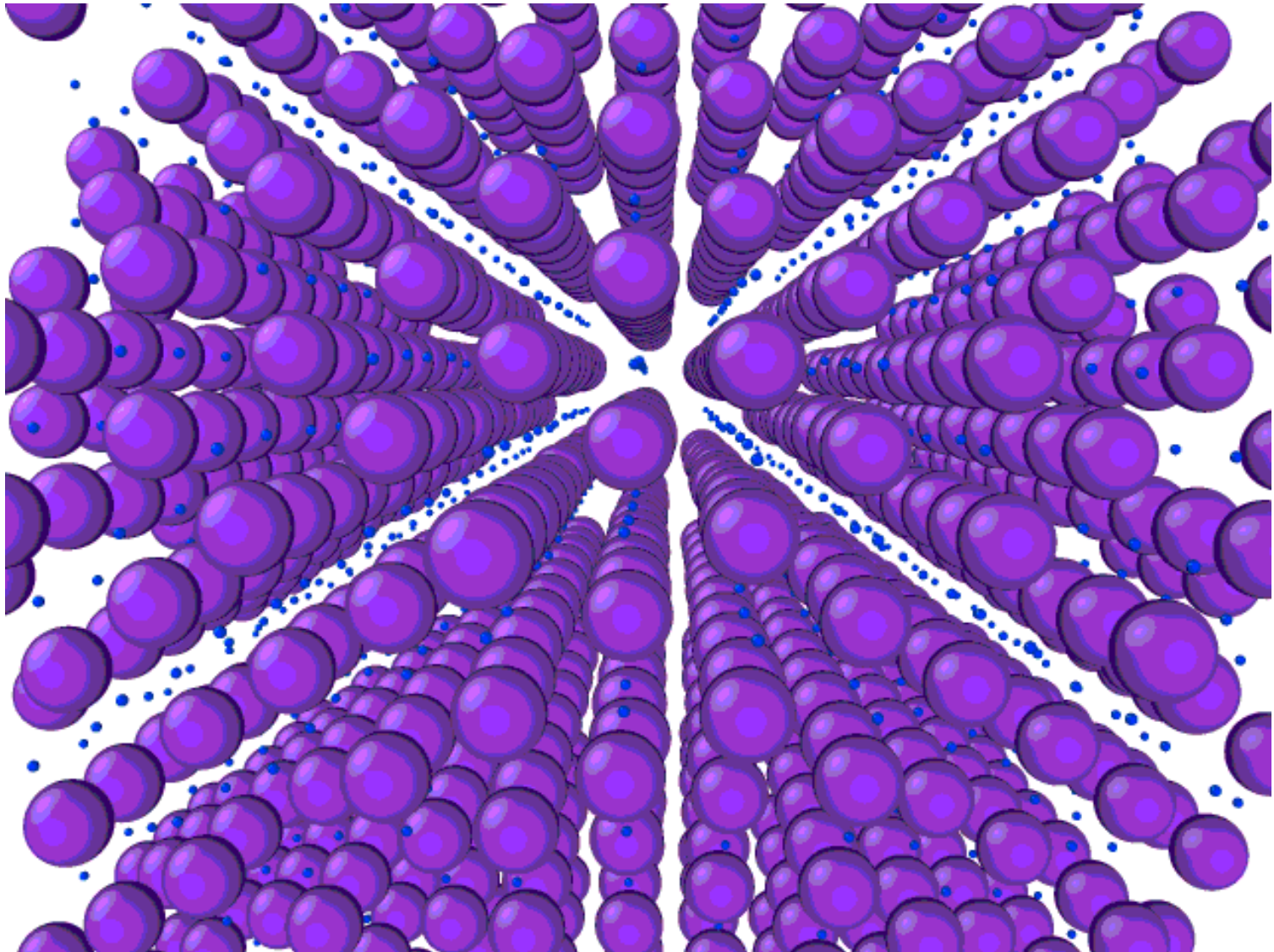


Do DBs exist at finite T ?

Visualization of the PdH fcc Lattice Oscillations at $T=100$ K

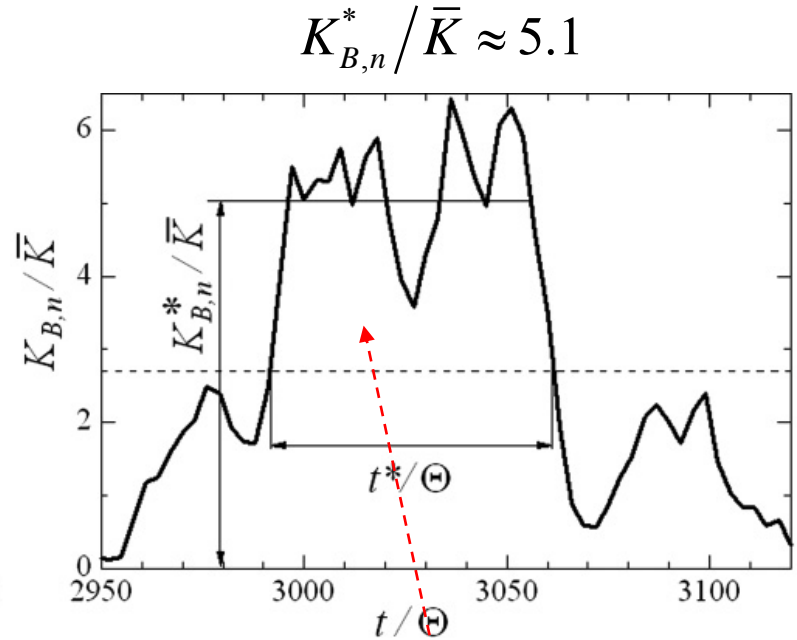
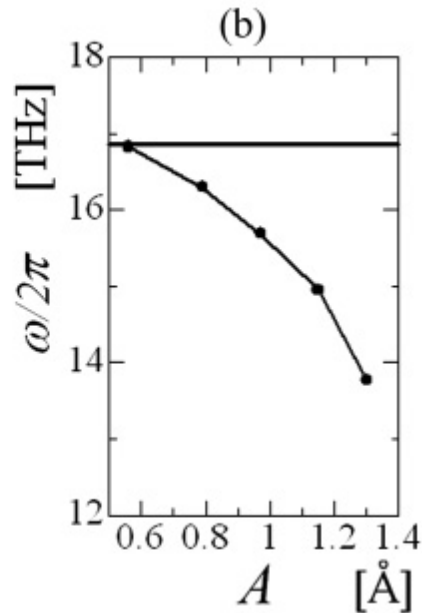
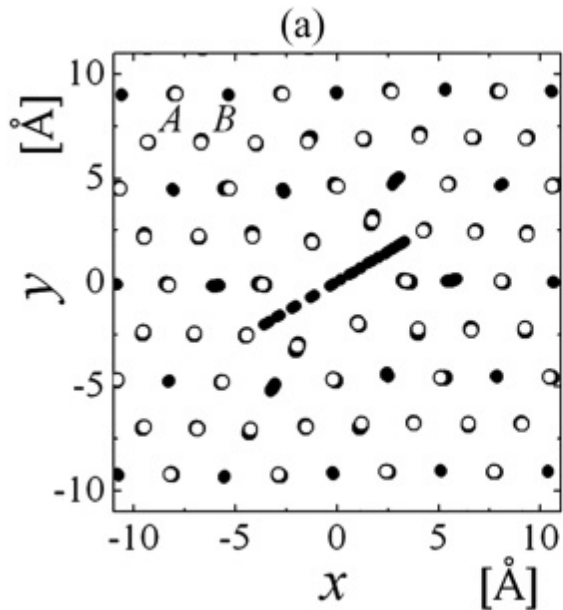


Visualization of the PdH fcc Lattice Oscillations at $T=1000\text{K}$



Gap DBs in diatomic crystals at elevated temperatures

Hizhnyakov et al (2002), Dmitriev et al (2010)

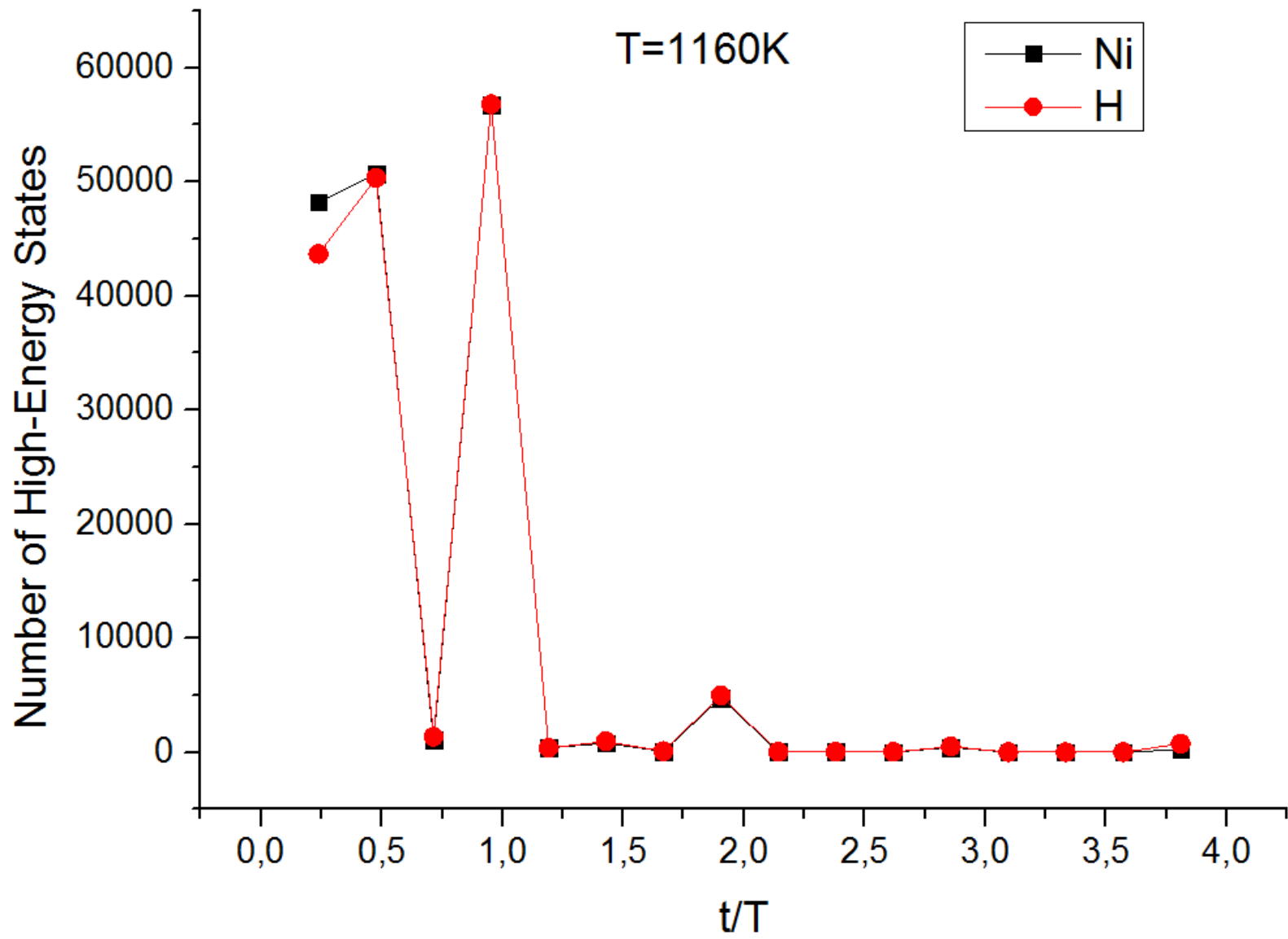


A_3B type crystals $M_H/M_L = 10$

$t^*/\Theta \approx 70 \bar{K} = 0.1eV \geq 1000K$

In NaI and KI crystals Hizhnyakov et al has shown that DB amplitudes along $\langle 111 \rangle$ directions can be as high as 1 \AA , and $t^*/\Theta \sim 10^4$

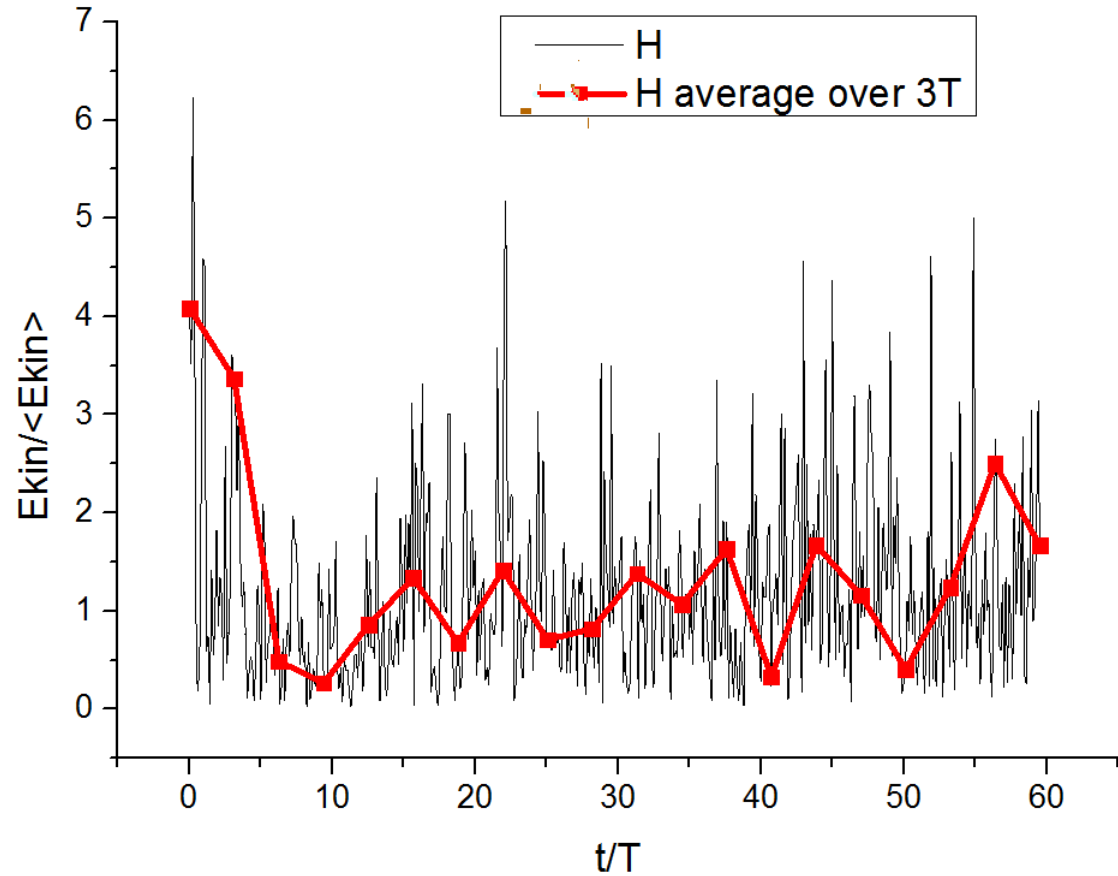
Lifetime and concentration of **high-energy light atoms** increase exponentially with increasing T



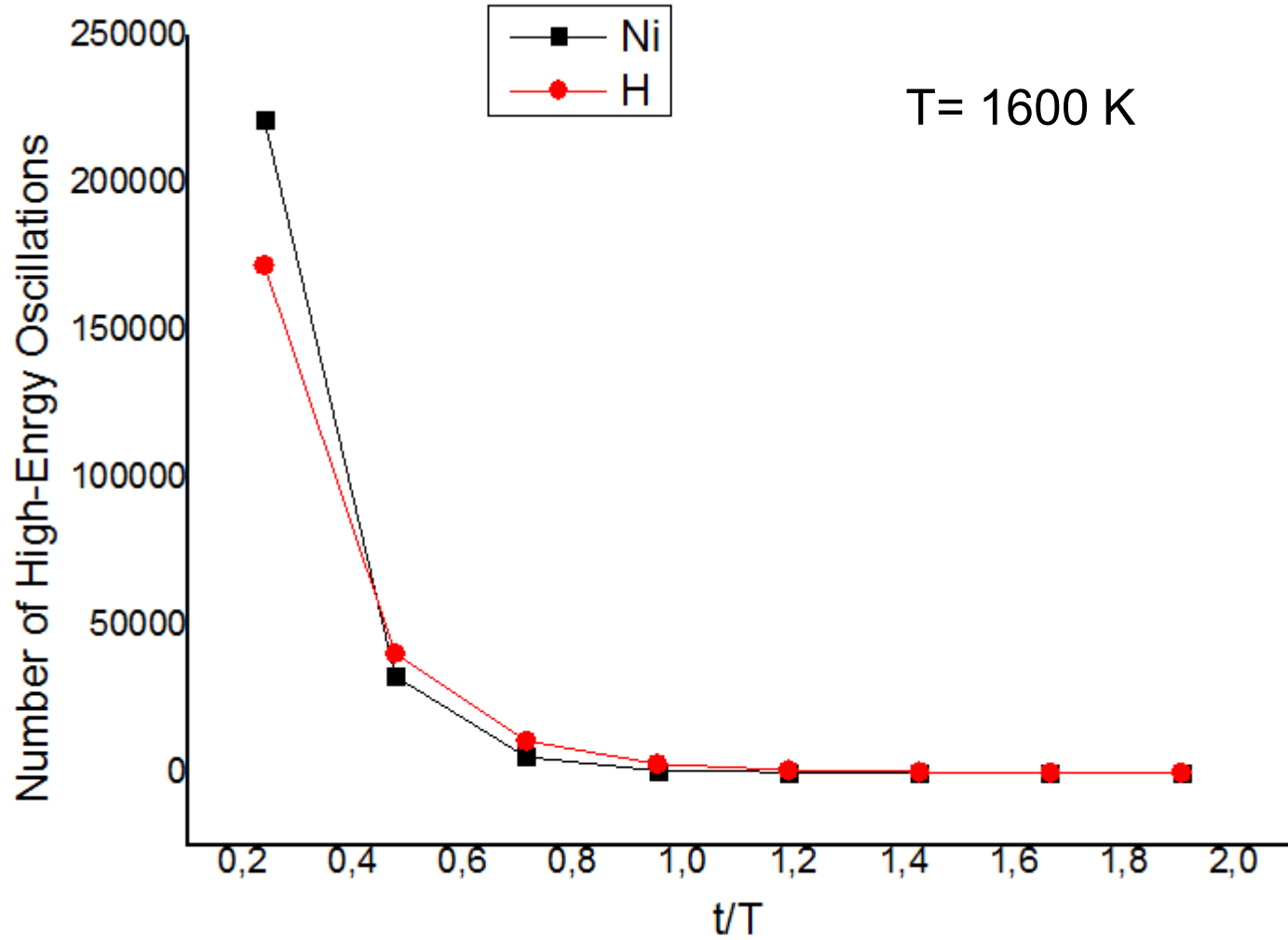
NiH MD modeling in LAMMPS package

NiH lattice at T=1160K. High energy oscillations

Data for some arbitrary H atom in the Lattice



NiH MD modeling in **LAMMPS** package

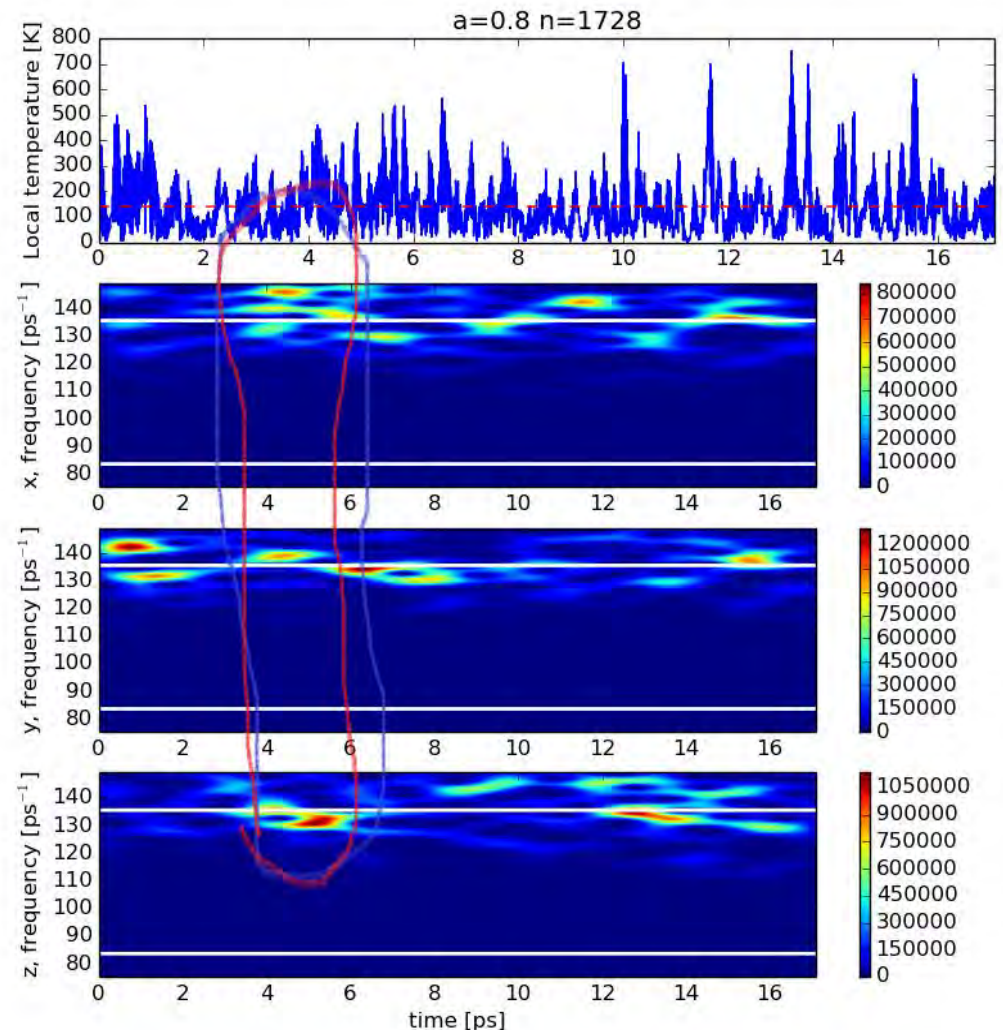


NiH MD modeling in **LAMMPS** package

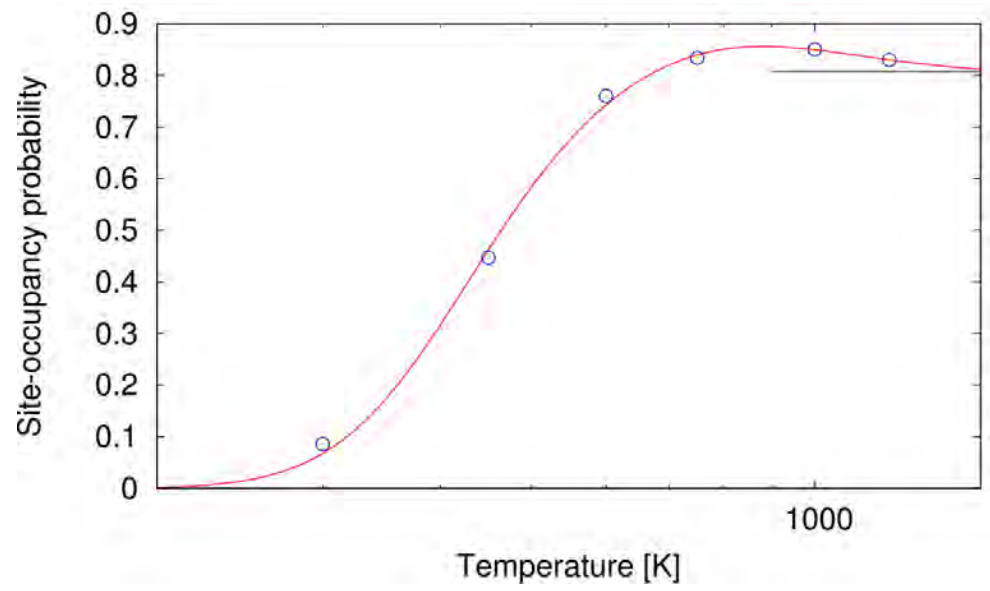
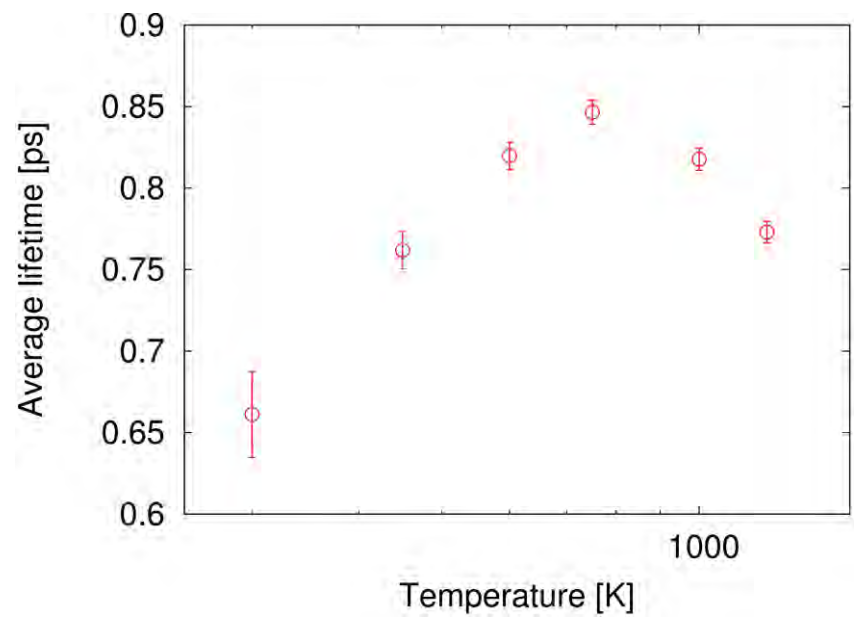
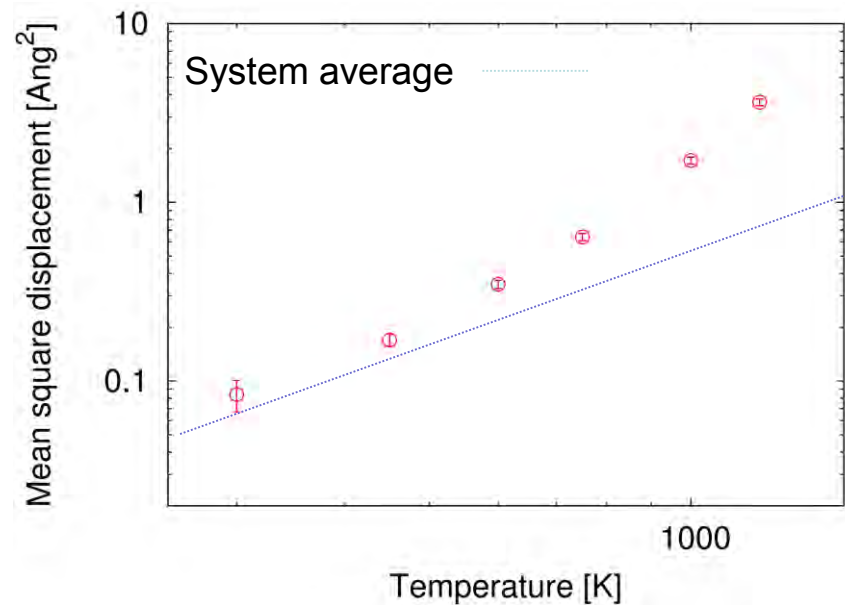
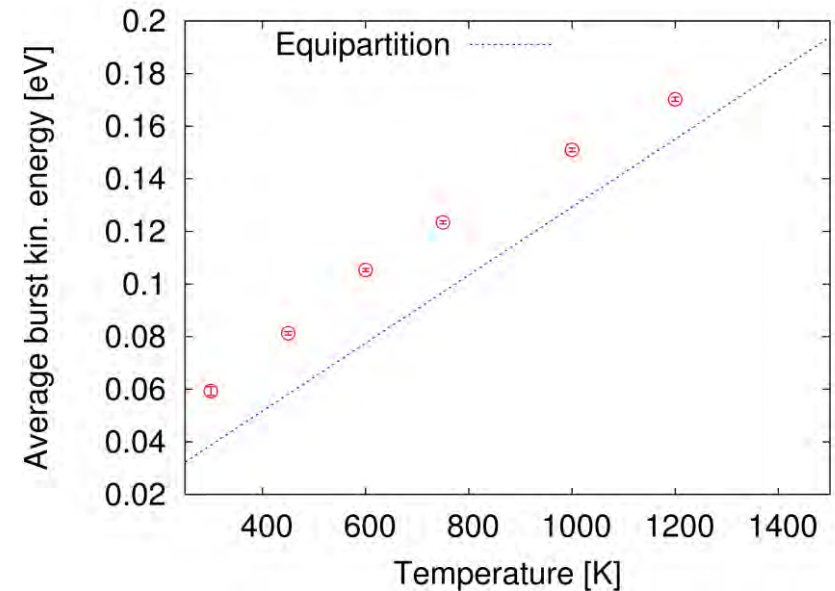
Wavelet imaging of LAV in NiH MD (Francesco Piazza, NaI, 2018)

The technique is based on continuous wavelet transform of velocity time series coupled to a threshold dependent filtering procedure to isolate excitation events from background noise in a given spectral region.

By following in time the center of mass of the reference frequency interval, the data can be exploited to investigate the statistics of the burst excitation dynamics, by computing, for instance, the distribution of the burst lifetimes, excitation times, amplitudes and energies.



Wavelet imaging of LAV in NiH MD (Francesco Piazza, 2018)



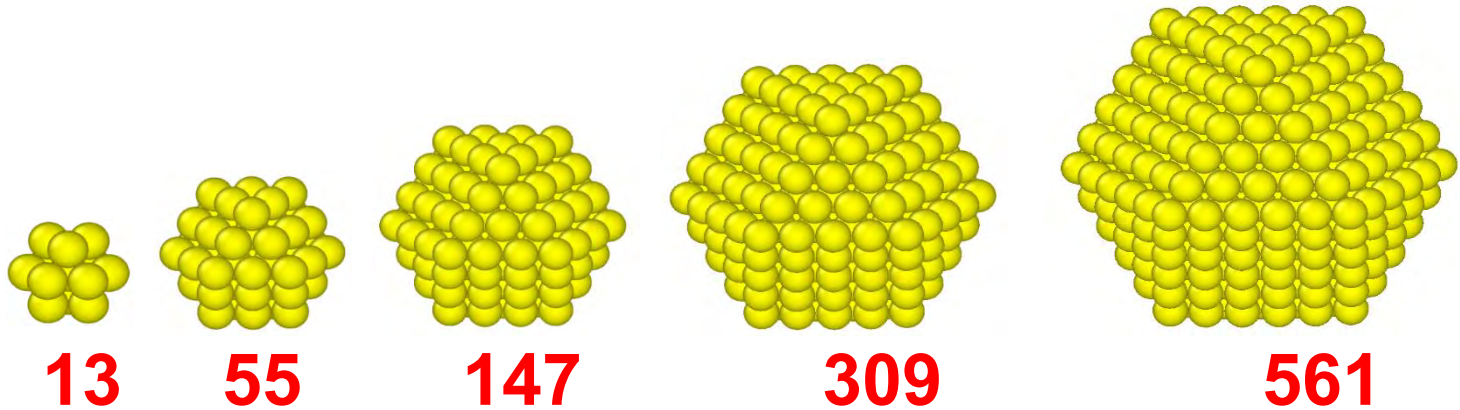
Nanoclusters

In physics, the term **clusters** denotes small, multiatom particles. As a rule of thumb, any particle of somewhere between 3 and 3×10^7 atoms is considered a cluster. Two-atom particles are sometimes considered clusters as well. A two atom particle may also be a molecule.

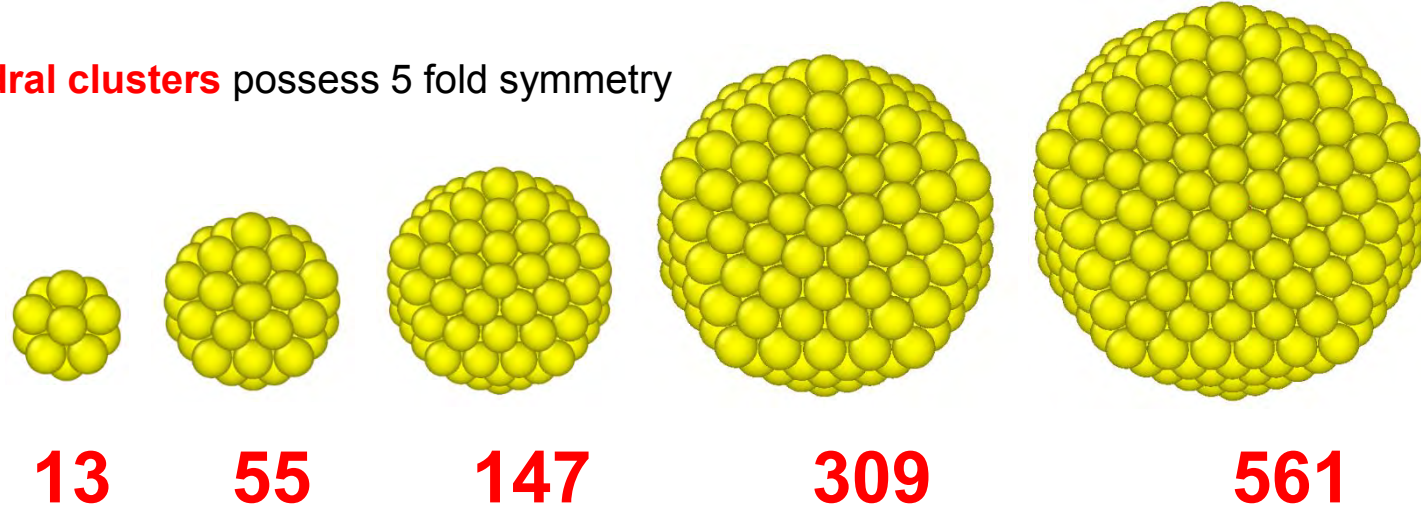
Nanoclusters are particles between 1 and 100 nanometers (nm) in size with a surrounding interfacial layer. The interfacial layer is an integral part of nanoscale matter, fundamentally affecting all of its properties. The interfacial layer typically consists of ions, inorganic and organic molecules. Organic molecules coating inorganic nanoparticles are known as stabilizers, capping and surface ligands, or passivating agents. In nanotechnology, a particle is defined as a small object that behaves as a whole unit with respect to its transport and properties.

Cuboctahedral and Icosahedral clusters

Cuboctahedral clusters (fcc) the only spatial configuration in which the length the polyhedral edges is equal to that of the radial distance from its center of gravity to any vertex



Icosahedral clusters possess 5 fold symmetry



Dependence of cluster **diameter** on number of atoms

# of atoms	d(Pd cubo), A	d(Pd ico), A	d(Ni cubo), A	d(Ni ico), A
13	4,90378	4,84784	4,70871	4,62434
55	10,0373	9,81988	9,51871	9,26282
147	15,286	14,9416	14,3779	13,958
309	20,6372	20,1318	19,2754	18,6855
561	26,0577	25,3113	24,1922	23,4326
923		30,5118		28,1917

CUBO-ICO Structural Transformation at near 0K

Unifying motion between 4-fold (crystal) and 5-fold (quasi-crystal) symmetries

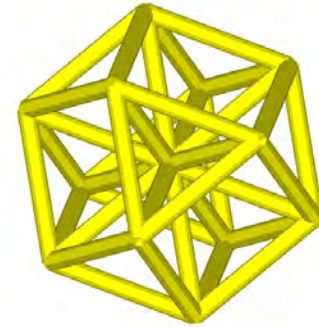
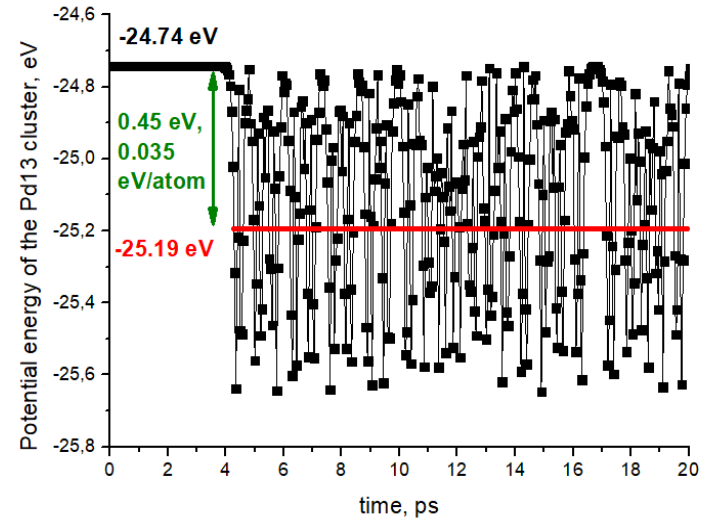
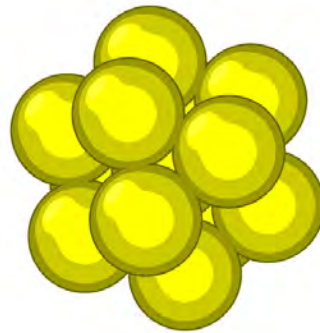
Reversible and irreversible



cuboctahedron

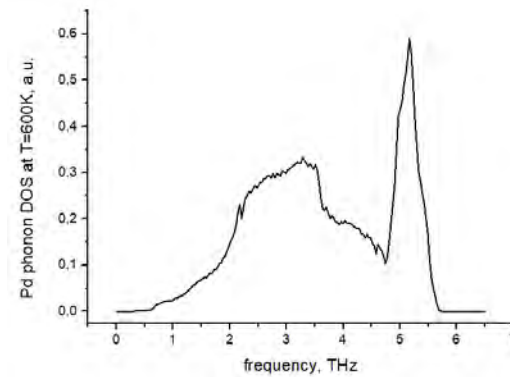
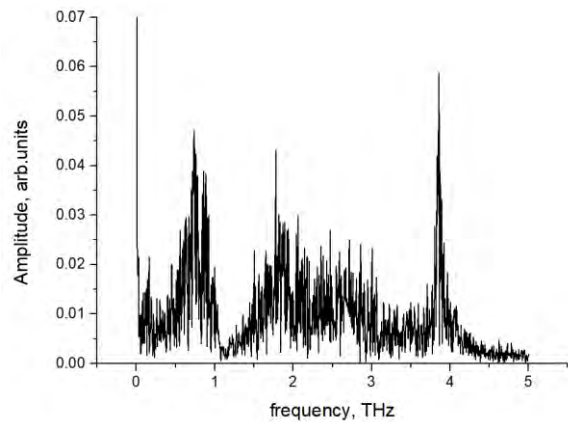
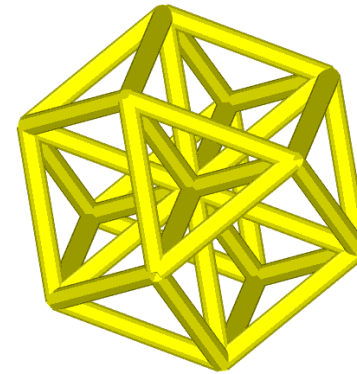
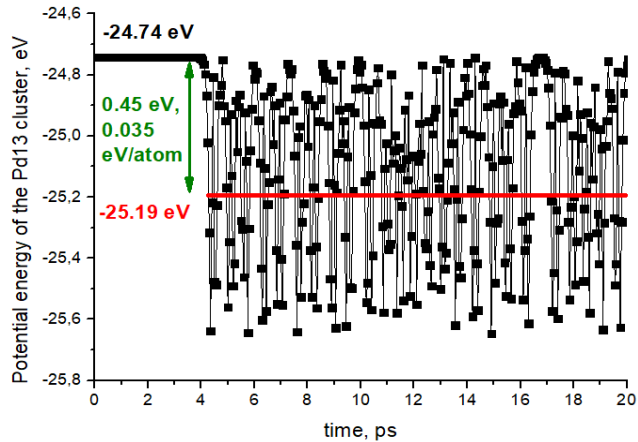


icosahedron

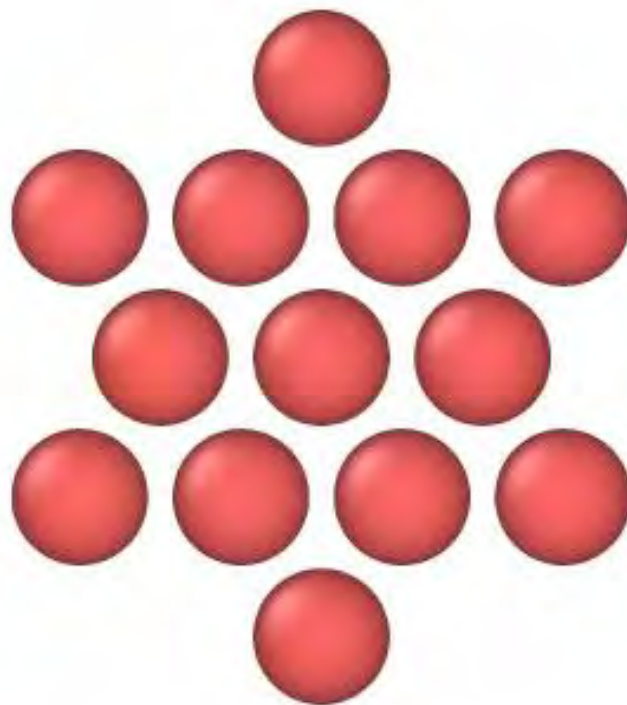


Time Dependence of Potential Energy for Pd13

For different clusters we analyzed the oscillations of potential energy.

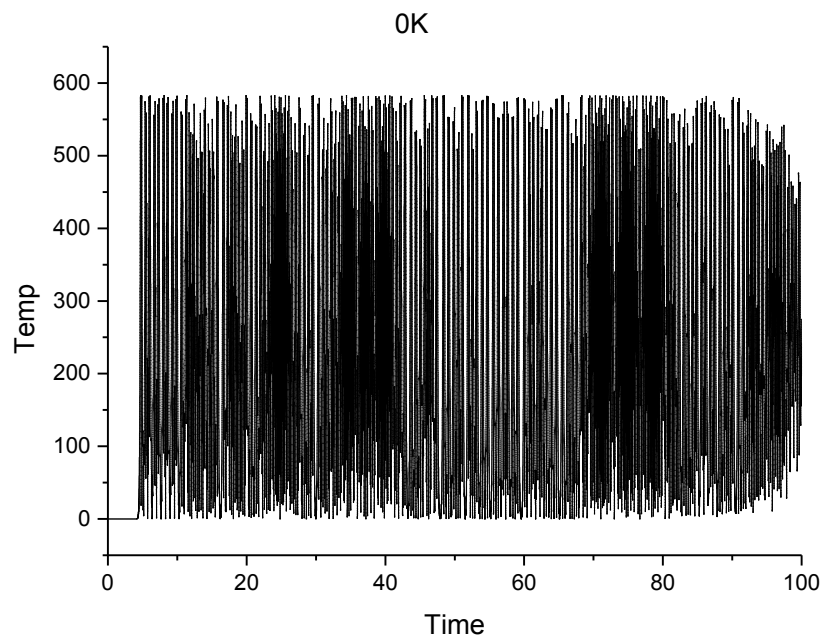
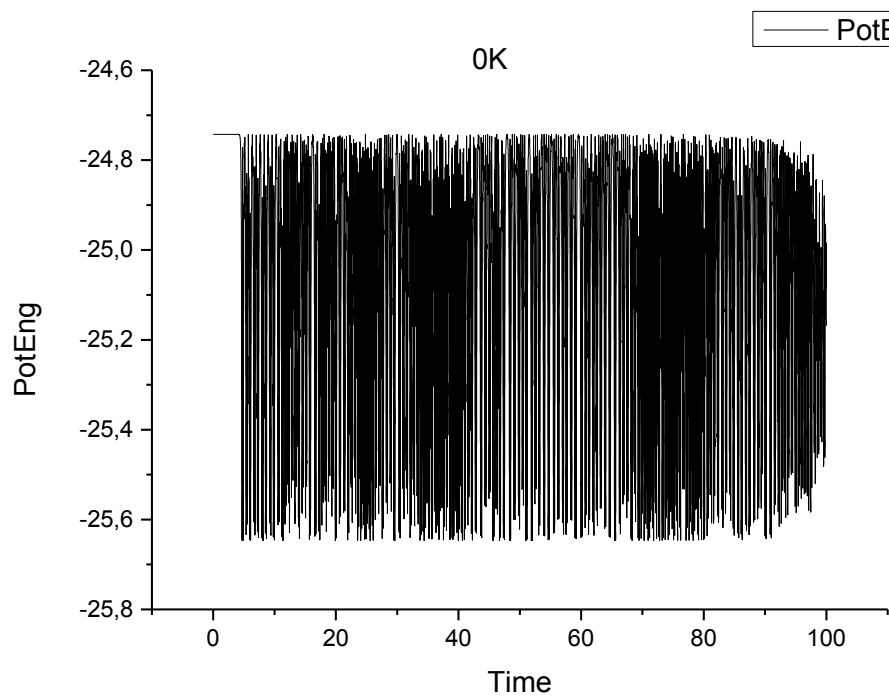


CUBO-ICO Structural Transformation at near 0K

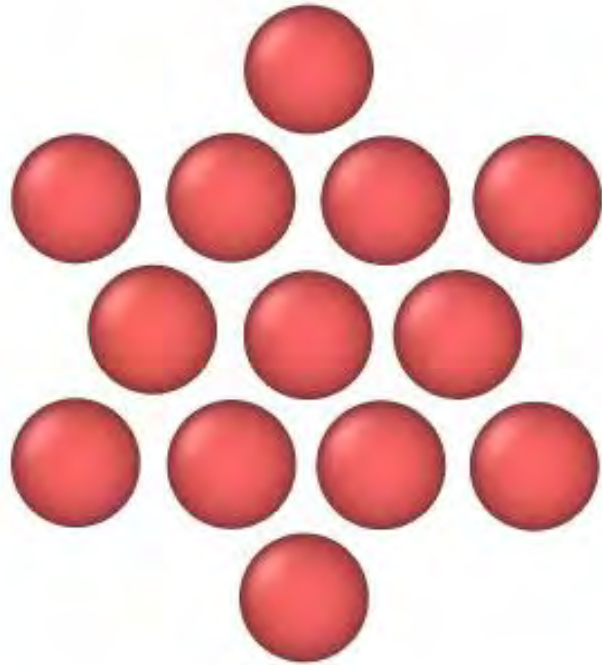


Pd13_cubo_nve

Pd13 CUBO cluster has been considered. Initial temperature was set to 0K. After that the NVE dynamics has been modeled. Time in picoseconds, energy in eV.

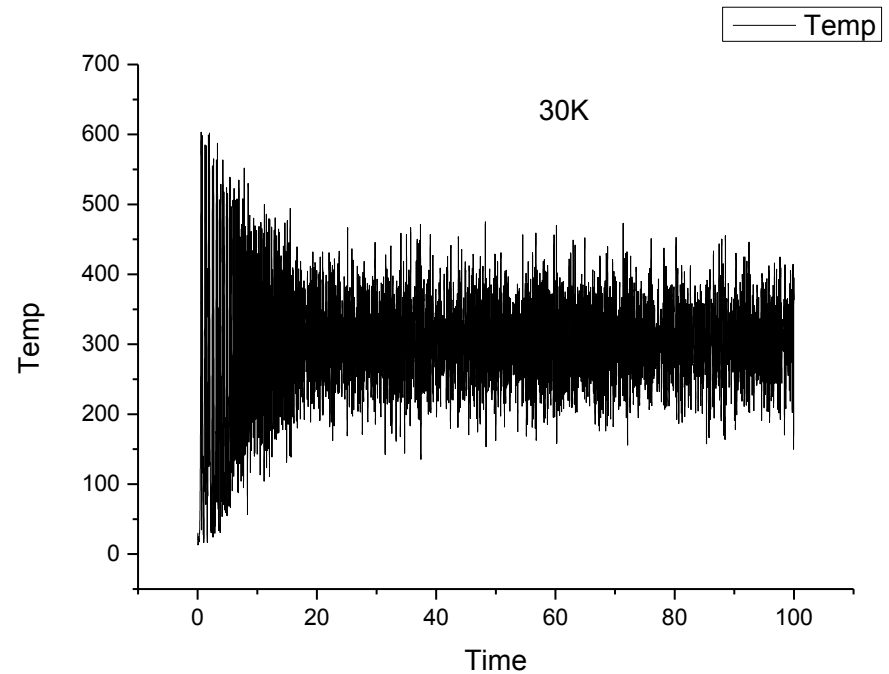
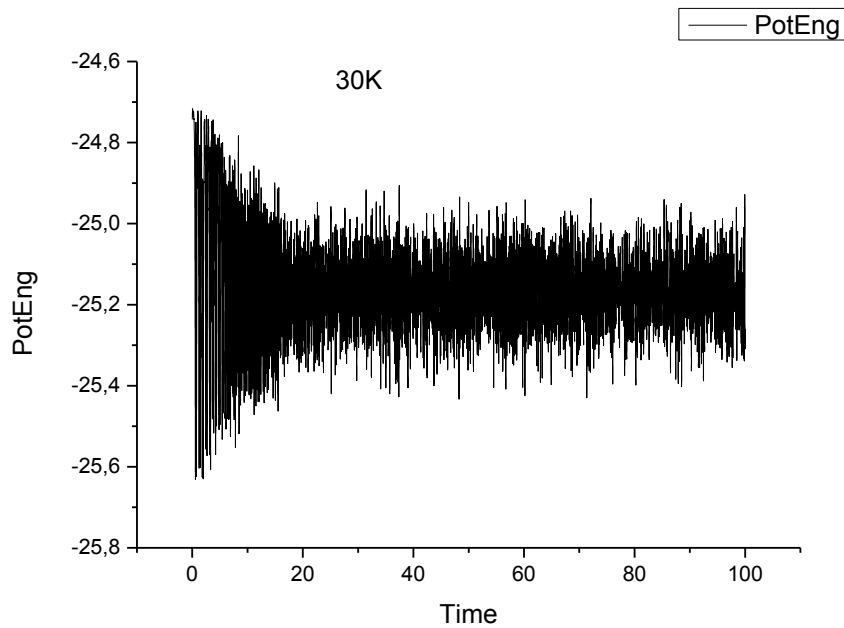


CUBO-ICO Structural Transformation at 30K

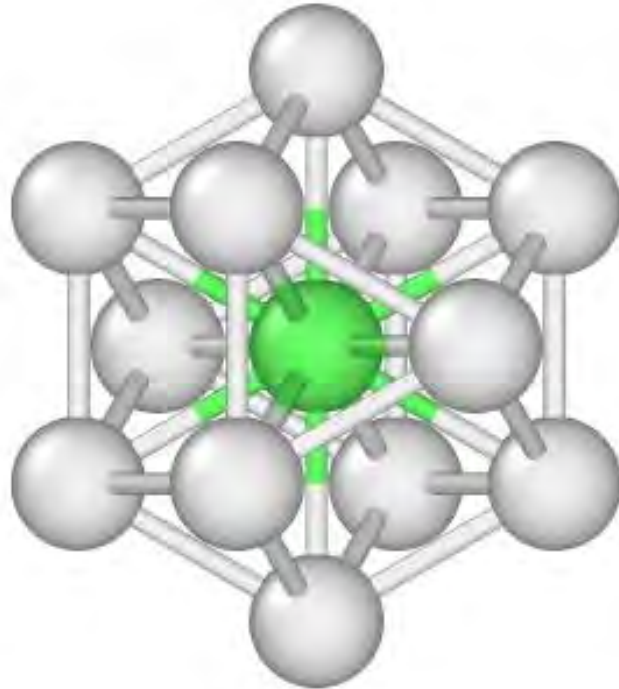


Pd13_cubo_nve

Pd13 CUBO cluster has been considered. Initial temperature was set to 30K. After that the NVE dynamics has been modeled. Time in picoseconds, energy in eV.

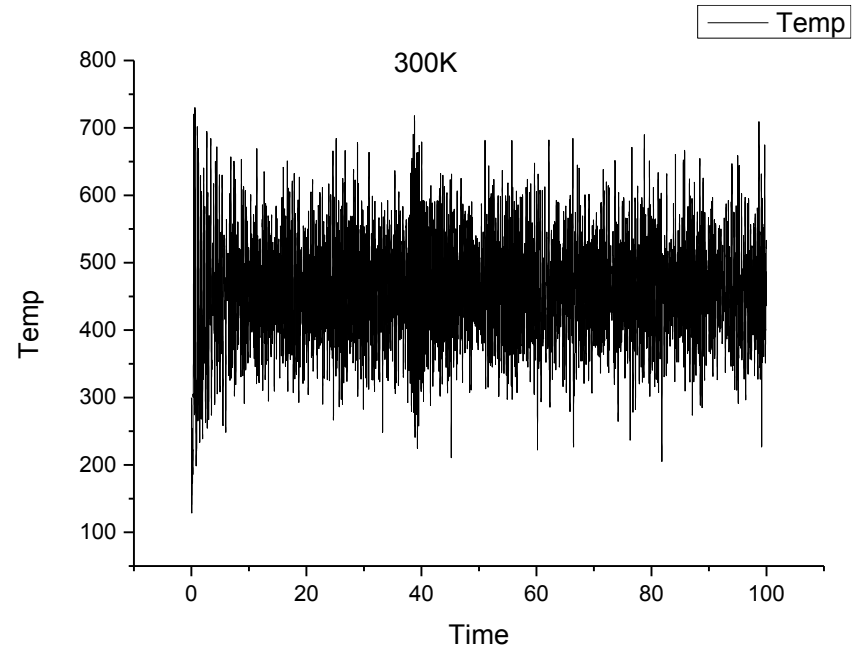
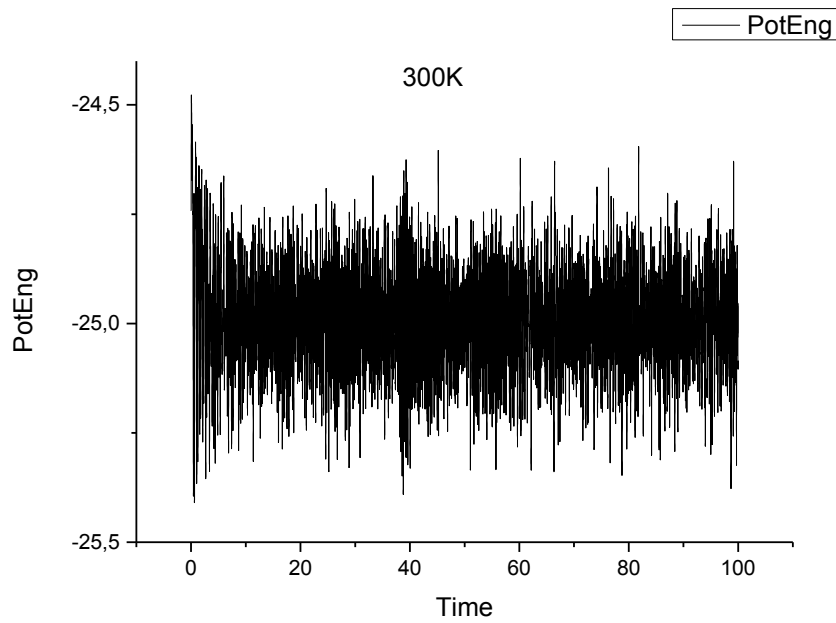


CUBO-ICO Structural Transformation at 300K



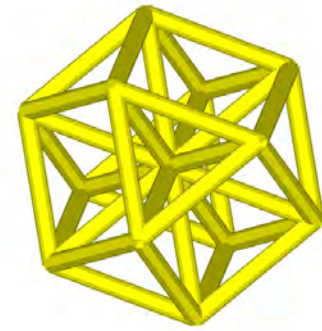
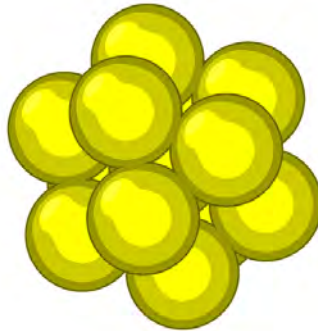
Pd13_cubo_nve

Pd13 CUBO cluster has been considered. Initial temperature was set to 300K. After that the NVE dynamics has been modeled. Time in picoseconds, energy in eV.



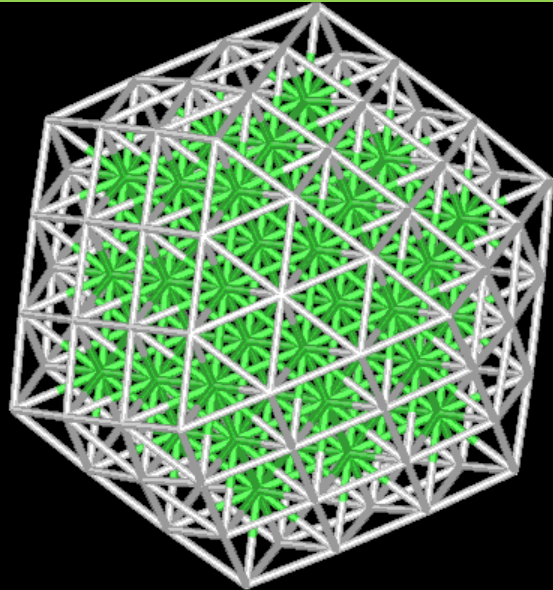
Temperature-driven phase transformation

- QCs of Pd exhibit temperature driven phase transformation
- Size of cluster and hydrogenization affects transformation
- Larger size – higher transformation temperature
- High Hydrogen concentration – lower transformation temperature

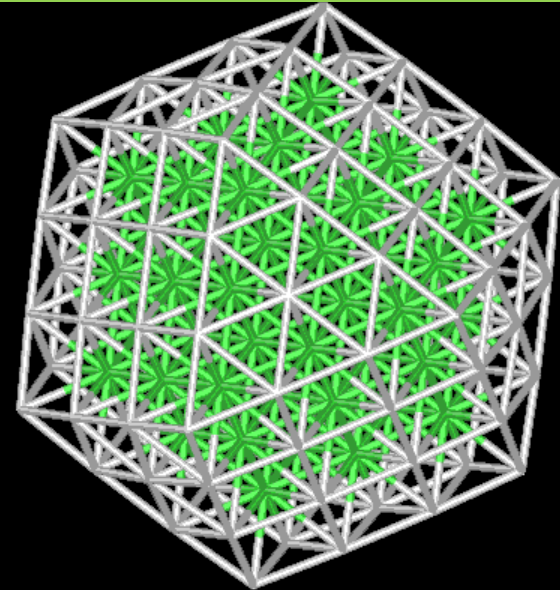


Temperature of the Structural Transition for Ni₁₄₇ cluster. T=133K

For larger clusters there exists some critical temperature for the transition. For Ni₁₄₇ Structural transition was observed at T=133K. For T<133K cuboctahedral cluster preserved its symmetry and didn't transform to icosahedral cluster



T=132K

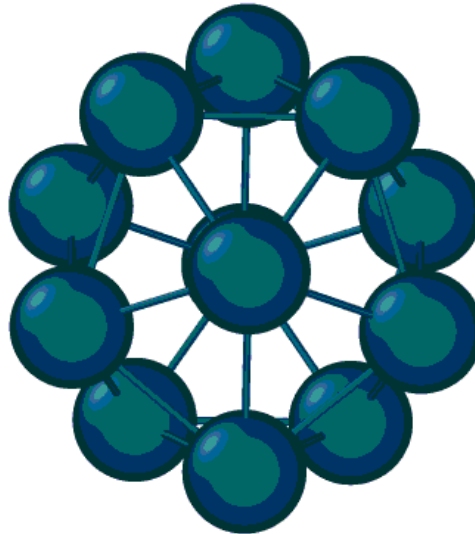


T=133K (Structural Transition)

MD modeling of the Pd-H and Ni-H clusters heating

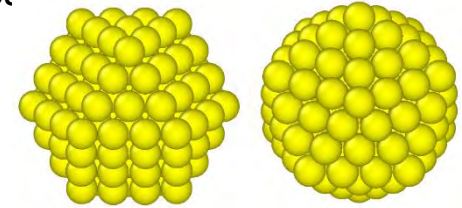
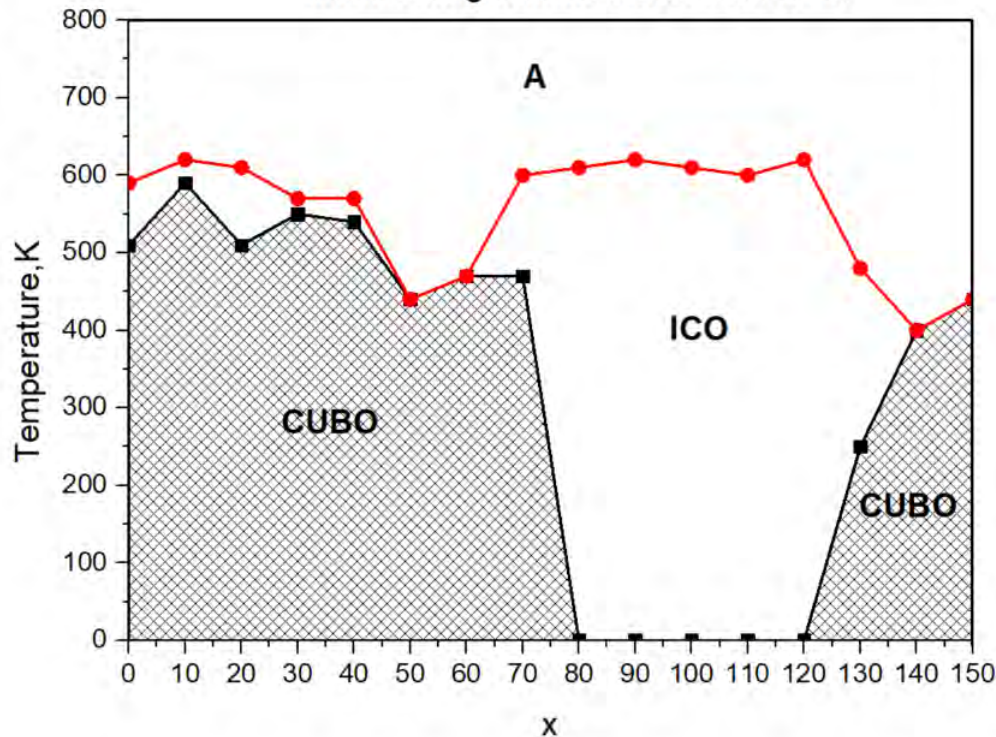
The heating of clusters was performed in a canonical (NVT) ensemble with Nose thermostat. During the simulation the temperature was determined by the average kinetic energy of the atoms, which was calculated using the Verlet velocity algorithm with a time step $0.0005\text{ps} = 0.5\text{fs}$.

During the heating the temperature was changed from 10 to 1000K



x-T Phase diagram for the Pd147Hx cluster

Initial condition: cluster has cuboctahedral (CUBO) configuration. The heating of clusters was performed in a canonical (NVT) ensemble with Nose thermostat. During the simulation the temperature was determined by the average kinetic energy of the atoms, which was calculated using the Verlet velocity algorithm with a time step $0.0005\text{ps} = 0.5\text{fs}$.



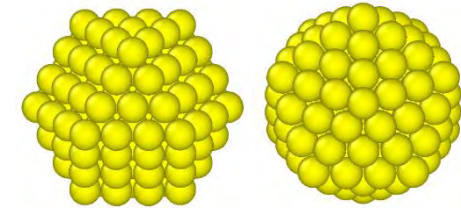
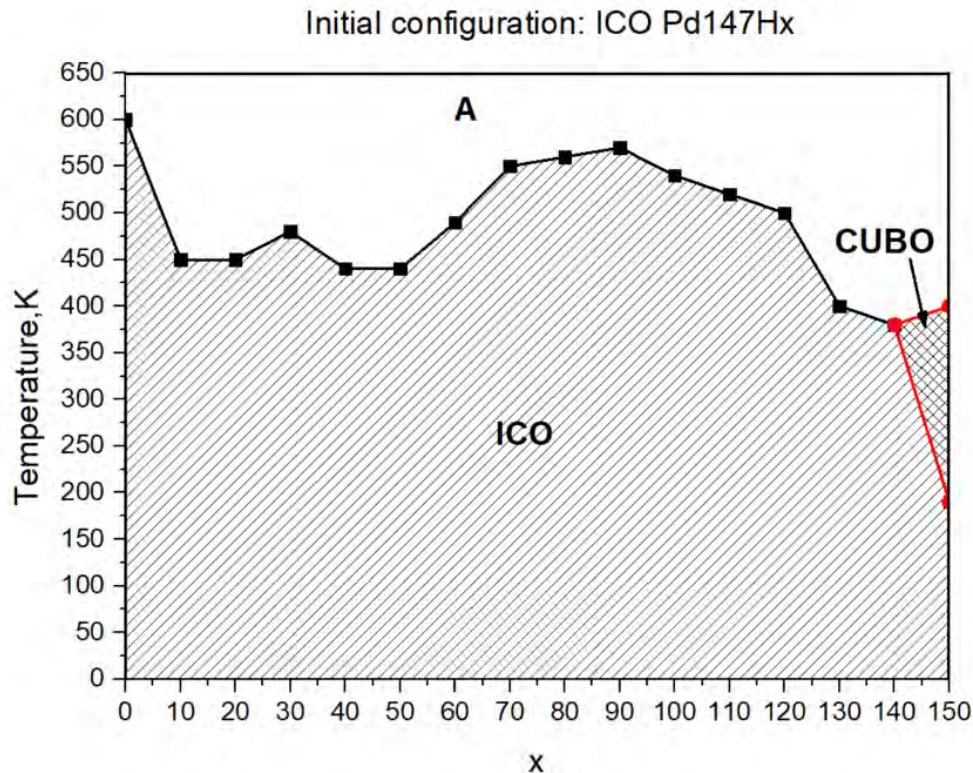
CUBO

ICO

As temperature (T) increase cluster undergoes transformation from cuboctahedral (CUBO) phase to icosahedral (ICO) phase and then to amorphous (A) phase. The further temperature increase results in melting and evaporation/sublimation processes. Clusters with different number of H atoms (x) have been considered.

x-T Phase diagram for the Pd147Hx cluster

Initial condition: cluster has icosahedral (ICO) configuration. The heating of clusters was performed in a canonical (NVT) ensemble with Nose thermostat. During the simulation the temperature was determined by the average kinetic energy of the atoms, which was calculated using the Verlet velocity algorithm with a time



CUBO

ICO

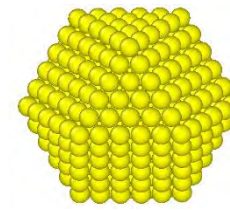
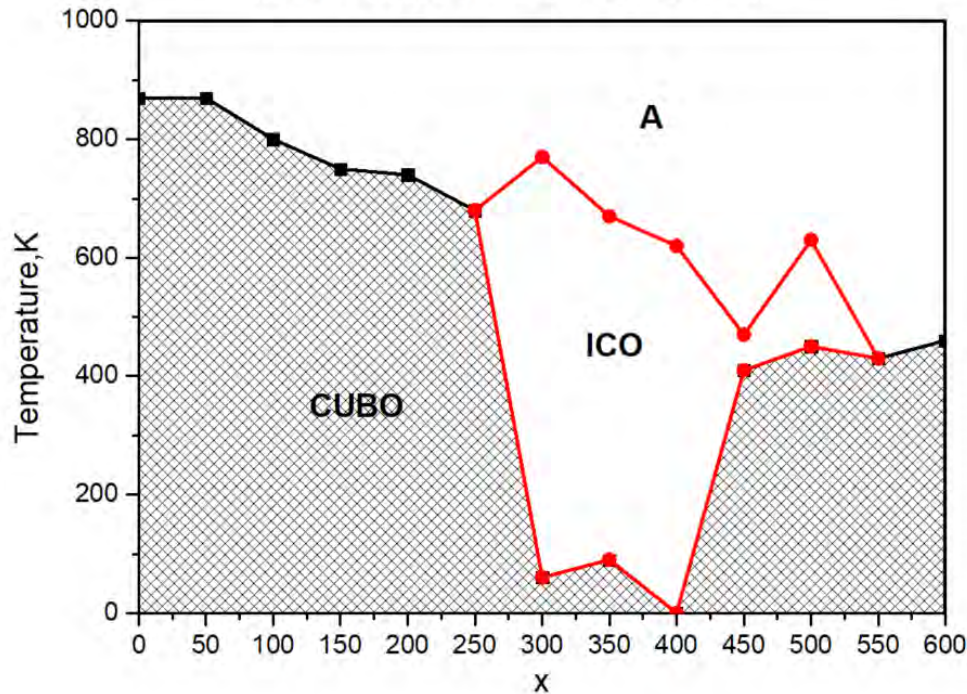
As temperature (T) increase cluster undergoes transformation from icosahedral (ICO) phase to amorphous (A) phase. The further temperature increase results in melting and evaporation/sublimation processes. Clusters with different number of H atoms (x) have been considered.

For large x the transformation to cuboctahedral (CUBO) phase was observed.

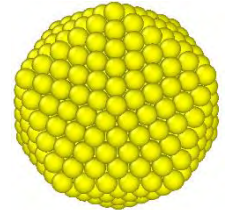
x-T Phase diagram for the Pd561Hx cluster

Initial condition: cluster has cuboctahedral (CUBO) configuration. The heating of clusters was performed in a canonical (NVT) ensemble with Nose thermostat. During the simulation the temperature was determined by the average kinetic energy of the atoms, which was calculated using the Verlet velocity algorithm with a time step $0.0005\text{ps} = 0.5\text{fs}$.

Initial configuration: CUBO Pd561Hx



CUBO

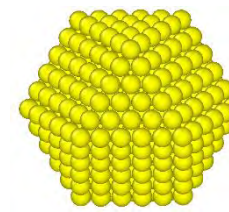
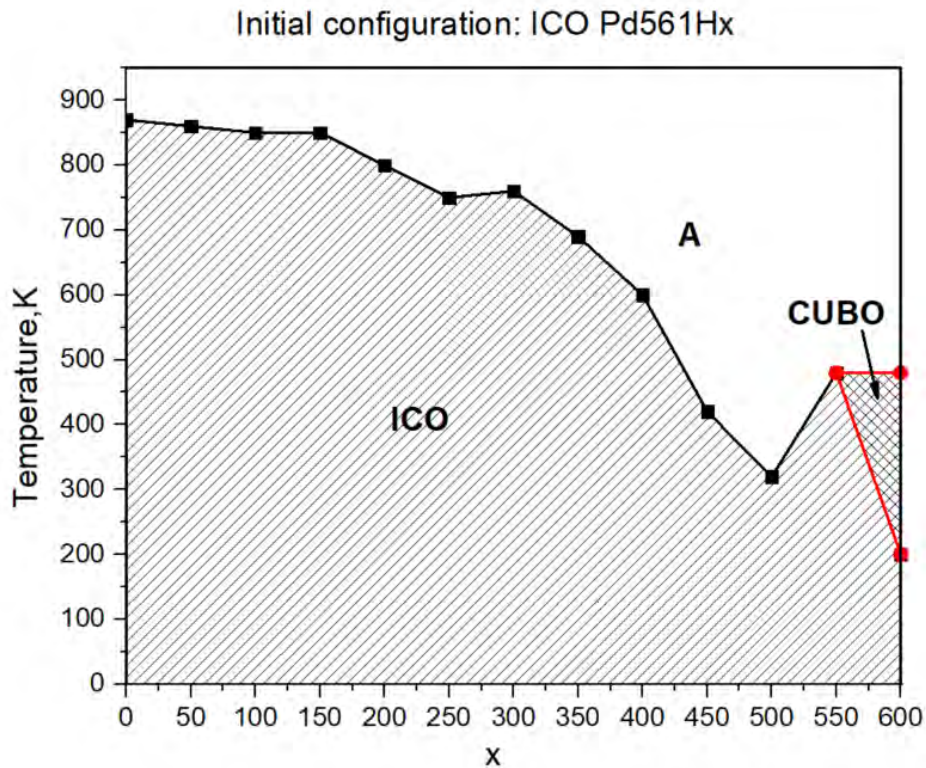


ICO

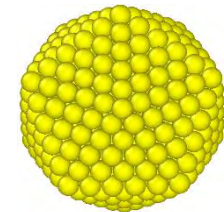
As temperature (T) increase cluster undergoes transformation from cuboctahedral (CUBO) phase to icosahedral (ICO) phase and then to amorphous (A) phase. The further temperature increase results in melting and evaporation/sublimation processes. Clusters with different number of H atoms (x) have been considered.

x-T Phase diagram for the Pd561Hx cluster

Initial condition: cluster has icosahedral (ICO) configuration. The heating of clusters was performed in a canonical (NVT) ensemble with Nose thermostat. During the simulation the temperature was determined by the average kinetic energy of the atoms, which was calculated using the Verlet velocity algorithm with a τ_{ii}



CUBO



ICO

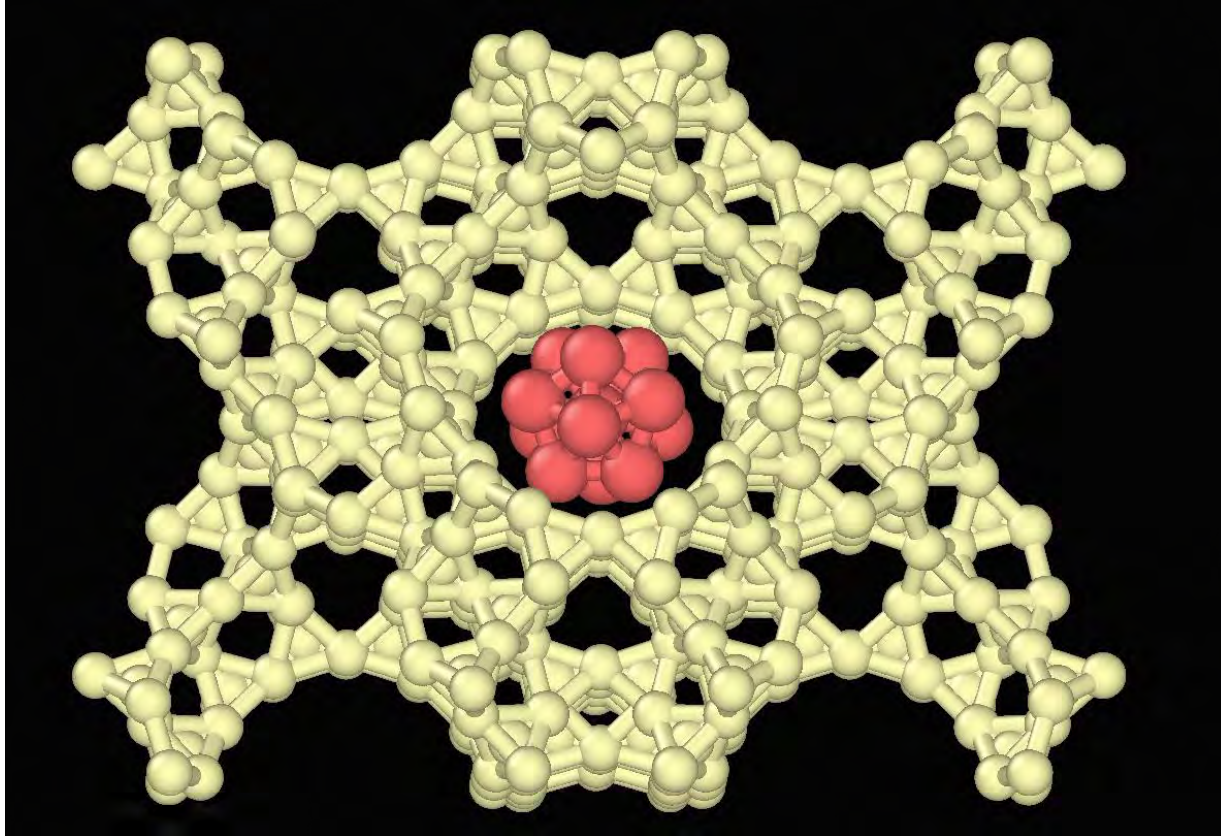
As temperature (T) increase cluster undergoes transformation from icosahedral (ICO) phase to amorphous (A) phase. The further temperature increase results in melting and evaporation/sublimation processes. Clusters with different number of H atoms (x) have been considered.

For large x the transformation to cuboctahedral (CUBO) phase was observed.

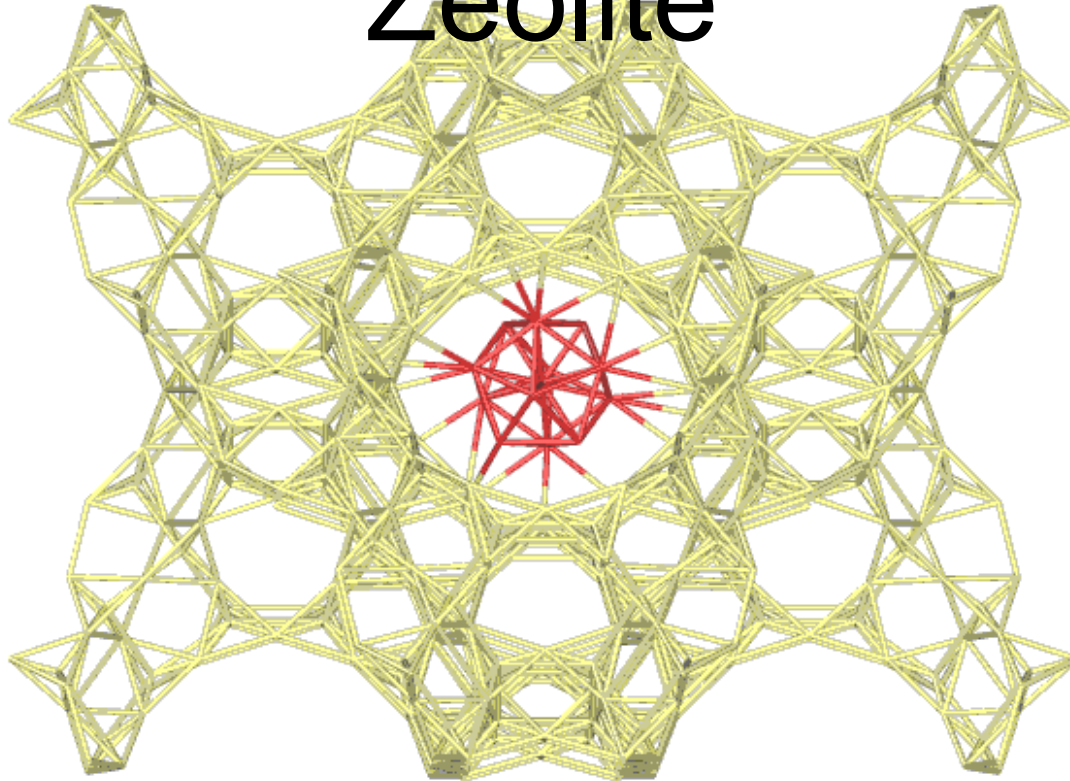
Embedding of QCs in Zeolite

- Strategy
 - Assumption: Zeolite act as “magnetic pillow” which holds QC
 - Phase transformation of QCs will occur in similar manner inside Zeolite just as in simulated vacuum
 - Atomic force interaction (Al-Si-O-H-Pd) can be derived from Ab Initio calculations and transferred to LAMMPs tool
- Current progress
 - Trial atomic force matrix is derived
 - Trial Zeolite – Pd 13 and Pd 147 is modelled
 - Phase transformation inside Zeolite is observed

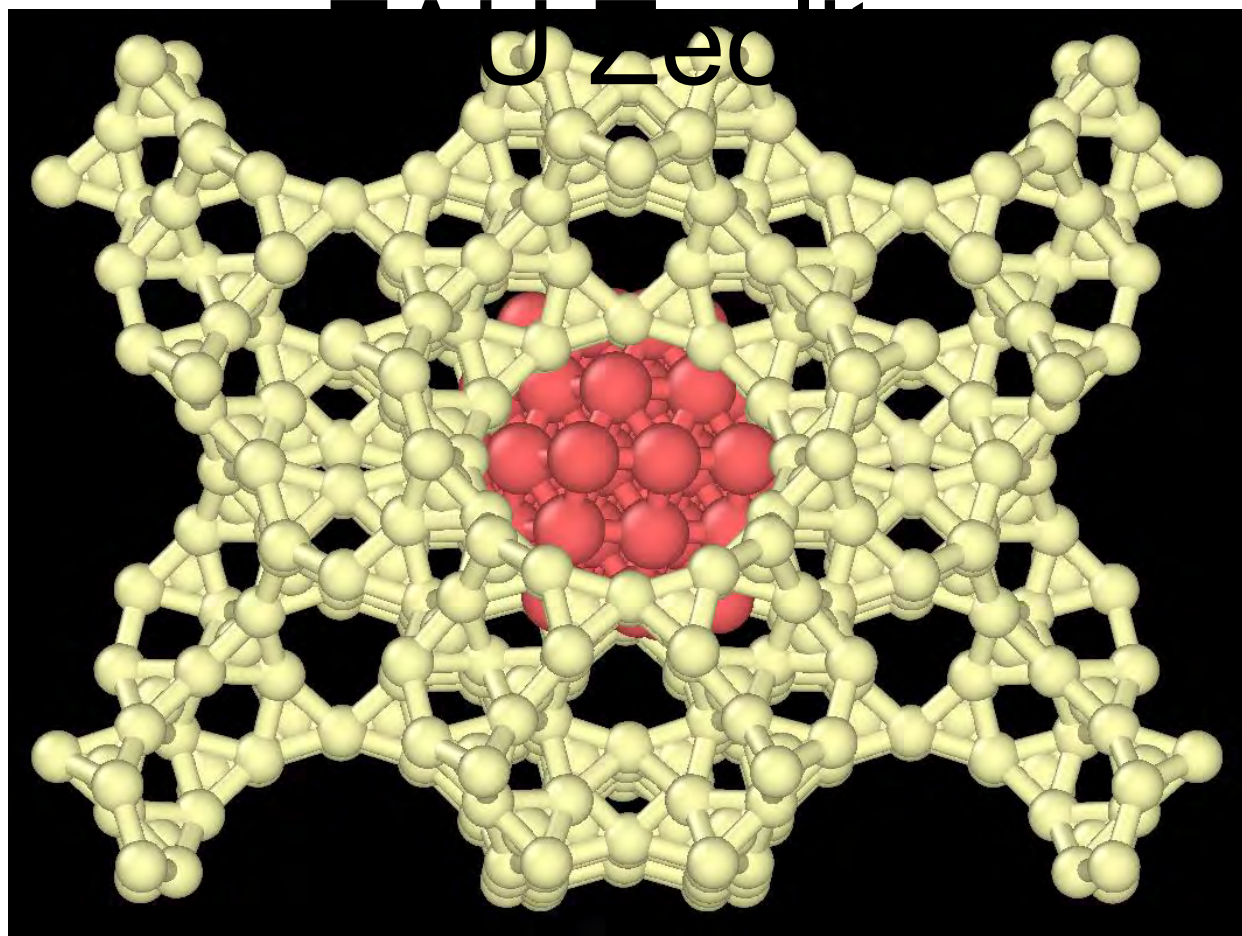
Pd₁₃ ICO cluster inside FAU Zeolite



Pd₁₃ ICO cluster inside FAU Zeolite



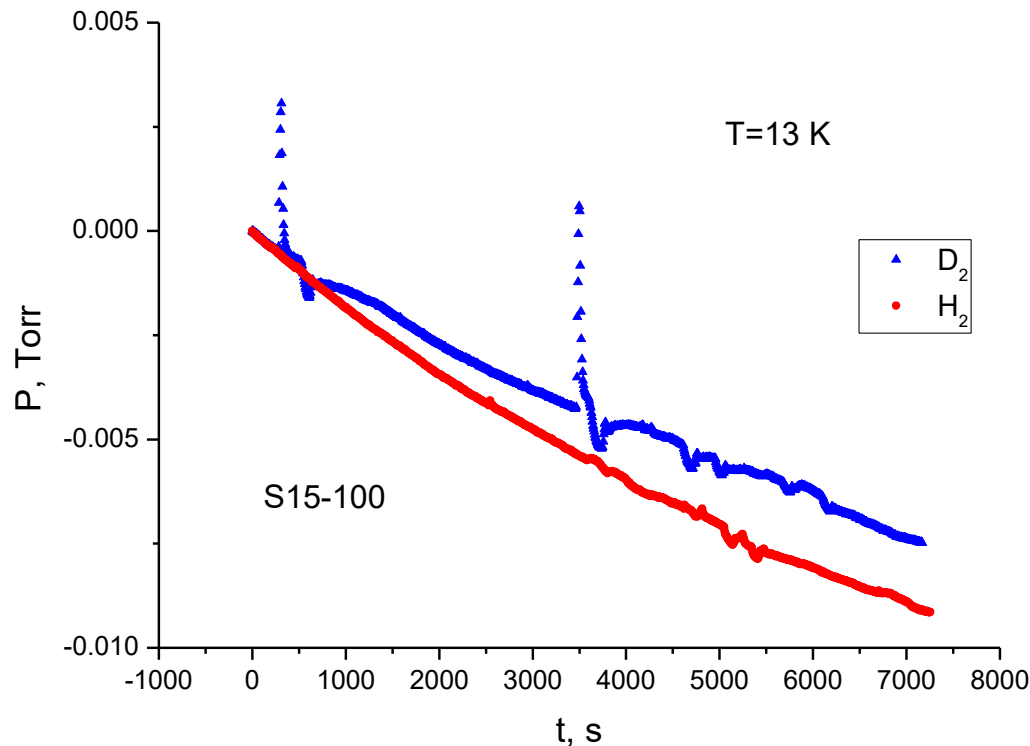
Pd₅₅ CUBO cluster inside



Summary

- Phason flip (or phase transformation of QC cluster) is considered as a possible trigger of D-D reaction
- Phason flip was modelled in Pd and Pd-H QC clusters by LAMMPS techniques; phase diagram is obtained for the QCs of relevant size and hydrogenization
- LAMMPS technique was validated by AB INITIO code to ensure that structure and energetic stability of QC clusters is respected
- Zeolite is now modelled as “Magnetic Pillow” holding the QC cluster
- Zeolite-QC cluster interaction matrix needs to be derived using AB INITIO, and then implemented in LAMMPS tool
- Preliminary calculations show that QCs embedded in Zeolite (with simplified force matrix) also exhibit phase transformation in similar style as observed by modelling “vacuum case”

Low temperature testing of the sample S14-100 (Carbon template with 15 wt% of 1.5-17 nm Pd nanoparticles)
By Prof. Alexander Dolbin, head of the [Department of Thermal properties and structure of Solids and nanosystems](#)
Kharkov Institute of Low Temperature Physics.



The hydrogen (red) and deuterium (blue) desorption curves from S14-100 sample at $T = 13$ K. Sudden bursts of gas pressure during desorption of deuterium at the beginning of desorption and after 3600 s can be seen far exceeds the experimental error. **A possible reason for the deuterium desorption bursts may be AHE bursts !!!**

Conclusions and outlook

New mechanism of catalysis in solids is proposed, based on **time-periodic driving** of the potential landscape induced by Discrete Breathers .

At high T, DBs formed in Pd or Ni hydrides may result in effective lowering of the reaction activation barrier.

At low T, DBs formed in Pd or Ni hydrides and Phason Flips of 13 atom Pd or Ni clusters may result in increasing energy of Zero Point Oscillations enhancing the tunneling through the potential barrier

Outstanding problems:

Efficient methods of DB generation in Pd or Ni hydrides are needed such as electromagnetic irradiation or electric pulses

Experimental methods to synthesize 13 atom Pd or Ni clusters (sizes ~ 0.5 nm!) confined in nano-porous matrixes need to be developed

Publications

1. V.I. Dubinko, P.A. Selyshchev and F.R. Archilla, *Reaction-rate theory with account of the crystal anharmonicity*, **Phys. Rev. E** 83 (2011),041124-1-13
2. V.I. Dubinko, F. Piazza, *On the role of disorder in catalysis driven by discrete breathers*, **Letters on Materials** 4 (2014) 273-278.
3. V.I. Dubinko, *Low-energy Nuclear Reactions Driven by Discrete Breathers*, **J. Condensed Matter Nucl. Sci.**, 14, (2014) 87-107.
4. V.I. Dubinko, *Quantum tunneling in gap discrete breathers*, **Letters on Materials**, 5 (2015) 97-104.
5. V.I. Dubinko, *Quantum Tunneling in Breather 'Nano-colliders'*, **J. Condensed Matter Nucl. Sci.**, 19, (2016) 1-12.
6. V. I. Dubinko, D. V. Laptev, *Chemical and nuclear catalysis driven by localized anharmonic vibrations*, **Letters on Materials** 6 (2016) 16–21.
7. V. I. Dubinko, *Radiation-induced catalysis of low energy nuclear reactions in solids*, **J. Micromechanics and Molecular Physics**, 1 (2016) 165006 -1-12.
8. V. I. Dubinko, D. V. Laptev, A. S. Mazmanishvili, J. F. R. Archilla, “*Quantum dynamics of wave packets in a nonstationary parabolic potential and the Kramers escape rate theory*”, **J. Micromechanics and Molecular Physics**, 1, 650010 -1-12 (2016)
9. Dubinko V., Laptev D., Irwin K., *Catalytic mechanism of LENR in quasicrystals based on localized anharmonic vibrations and phasons*, **J. Condensed Matter Nucl. Sci.** -2017.-V. 24.- P. 1-12
10. V. Dubinko, D. Laptev, D. Terentyev, S. V. Dmitriev, K. Irwin, *Assessment of discrete breathers in the metallic hydrides*, **Computational Materials Science** 158 (2019) 389–397

**THANK YOU
FOR YOUR ATTENTION!**